

## Kinetics of void formation in strained metals

J. KRZEMIŃSKI (WARSZAWA)

AN EXTENDED theory of void formation in strained metals is proposed. The theory takes into account the coupling of both homogeneous and heterogeneous mechanisms in the global process of vacancy-microvoid nucleation as well as the effect of strain on the free energy of formation of vacancy clusters. Moreover, numerical estimates of nucleation characteristics for two f.c.c. metals (aluminium and copper) and one b.c.c. metal ( $\alpha$ -iron) are presented and discussed.

Praca zawiera rozszerzoną teorię tworzenia pustek w odkształconych metalach. Teoria uwzględnia zarówno sprzężenie obu mechanizmów jednorodnego i niejednorodnego, w globalnym procesie zarodkowania wakansyjnych mikropustek, jak i wpływ odkształcenia na energię swobodną tworzenia agregatów wakansji. Ponadto przedstawiono i przedyskutowano oszacowania liczbowe charakterystyk nukleacyjnych dla dwóch metali o sieci płasko centrowanej (aluminium i miedź) oraz dla jednego metalu o sieci przestrzennie centrowanej (żelazo  $\alpha$ ).

В работе представлена теория образования пустот в деформируемых металлах. Теория учитывает как обратную связь обоих механизмов однородного и неоднородного в глобальном процессе зарождения вакансионных микропустот, так и влияние деформации на свободную энергию создания агрегатов вакансий. Кроме того, представлены и рассмотрены численные оценки нуклеационных характеристик для двух металлов с границентрированной решеткой (алюминий и медь), а также для одного металла с объемцентрированной решеткой ( $\alpha$ -железо).

### 1. Introduction

IT IS WELL known that metals and alloys develop an internal porosity in the form of small cavities when they are strained in tension at elevated temperatures [1], exposed to high-energy radiation [2, 3] or subject to diffusion experiments [4, 5]. Such cavities were shown to be essentially empty and were therefore called "voids". Although the phenomenon of void formation is a topic of immense interest to both theoretical and experimental physicists concerned with fracture, it has been considered only in recent years, and is still far from being fully understood.

In the preceding papers [6-11], a hypothesis of vacancy-microcrack origination in strained metals was proposed. The hypothesis was based on the qualitative similarity between the Griffith theory of brittle fracture and the process of phase transition. This similarity suggested the idea that a microcrack may be initiated in an analogous manner as a nucleus of a new phase, composed of a set of vacancies situated at neighbouring lattice points, and resembling a bubble in cavitation of liquids.

The vacancy hypothesis has been developed by the present author since 1969. First, using the discrete analysis of the classical theory of phase transitions, the homogeneous nucleation rate of microcracks in a uniaxially strained single crystal was derived [6, 7]. Then the theory was extended to polycrystalline materials and the heterogeneous nuclea-

tion of microcracks at the grain boundaries was described. In the latter problem two different analytical treatments of the process were distinguished. The first one permitted introduction of macroscopic parameters, and hence a thermodynamic model of the system [8]. On the other hand, for very small nucleus sizes application of the bulk variables was highly questionable and the use of microscopic quantities (and so of an atomistic model) was required. In this case the considerations were carried out on the basis of statistical mechanics [9]. Next, the continuum approach to the kinetics of the homogeneous process of microcrack nucleation in single crystals was presented [10]. The continuum analysis gave the same nucleation rate equation as that obtained by the discrete method, but the unknown non-equilibrium density of vacancy clusters was also found.

In the theories of phase transitions two basic classes of the processes are usually distinguished: homogeneous and heterogeneous nucleation. In nearly all hitherto existing theories one separate mechanism only, of the new phase nucleus generation, has been considered. For the homogeneous nucleation this is a spatial mechanism (three-dimensional diffusion of single structural elements) which allows to form a nucleus of the new phase within a mother phase. On the other hand, in the case of heterogeneous nucleation on an interface (e.g. condensation of vapours on a solid substrate) surface diffusion is considered to play the decisive role. In spite of a large number of papers on nucleation theory very little attention has been paid to what happens when both the homogeneous and heterogeneous mechanisms operate simultaneously [12–16]. However, both of the above mentioned mechanisms are really coupled in any process of heterogeneous nucleation on a foreign surface, and the total nucleation rate is not a simple sum of the two rates calculated for independent mechanisms. The problem of coupling of these two mechanisms in the global process of vacancy-microcrack formation in uniaxially strained metals was solved in ref. [11]. The purpose of this paper is to take into consideration not only the coupling of the homo- and heterogeneous mechanisms but also the effect of strain on the free energy of formation of vacancy clusters. Moreover, some numerical estimates are presented and important qualitative and quantitative conclusions are drawn. In the considerations macroscopic thermodynamic properties are ascribed to the subcritical and critical clusters, the continuum analysis of the process kinetics is employed, and isothermal state of the system is assumed.

## 2. Model of the system

When the gaseous phase of vacancies (“vacancy vapour”), contained within the grain space, comes into contact with the grain boundary, a phenomenon of vacancy deposition appears on the surface of the boundary. By analogy to the process of physical adsorption of a gas on a solid substrate this phenomenon is called adsorption of vacancies on the grain boundary, and the adsorbed vacancies are called advacancies. The reverse process is called desorption of vacancies.

Let us consider an internal region of a polycrystalline sample subject to tension and kept in a uniaxial state of strain. The observed region contains at least one grain (with its boundary) which together with all separate vacancies (phase I), dispersed inside the

grain space or adsorbed on the grain boundary, as well as all types of vacancy aggregations (phase II) — constitutes our system (Fig. 1). Within the grain isotropic clusters (microvoids, assumed as spherical) are formed according to the homogeneous mechanism and under the classical assumption that particular aggregates can grow or disintegrate only by successive associations or separations of single vacancies. At the same time, on the grain boundary heterogeneous cap-shaped islands are created by two different simultaneously operating mechanisms: by direct addition of individual vacancies from the grain space to the already existing clusters, and by successive joining of separate vacancies via surface diffusion along the boundary.

The smallest clusters of both types with equal probability of growth or disintegration are called the critical clusters or microcrack nuclei.

When the linear strain of the analysed crystal sample is equal to zero the system considered is in the thermodynamic equilibrium and the two phases can remain in stable equilibrium with each other for any length of time. Increasing the strain increases the supersaturation and throws the system out of this equilibrium but it is assumed that after a negligibly short time delay, for each given temperature  $T$  and a fixed strain  $\varepsilon$ , a new metastable equilibrium is recovered. This, in fact unstable, pre-transition state can be preserved for a certain time depending on the velocity of the generation and growth of the new phase. Thus, any analysis of a system being in such a condition can yield results which are valid for a limited lapse of time only. Similarly as in the ordinary thermodynamic equilibrium quasi-stability of the system is expressed in this case by the steady character of the distribution of the new phase embryonic elements. As the strain increases further the system becomes considerably supersaturated with vacancies and aggregates of perceptible sizes are generated. Finally, when the strain is high enough, and correspondingly the degree of supersaturation, critical aggregates are also nucleated.

From the above it follows that two of the cluster distributions are of importance. The first one is an equilibrium distribution of clusters and holds true from the initial stage of the process to the highest supersaturation of the system at which the nucleation rate is still negligibly small. For higher supersaturation the new phase begins already to form, the first nuclei appear, and the equilibrium concentration of various classes of clusters redistribute to a new non-equilibrium distribution which after a short time delay attains again a steady state.<sup>(1)</sup>

In our considerations we limit ourselves to such a time interval of the phenomenon observation which lasts from the initial stage of the process ( $\varepsilon = 0$ ) to the time of formation of the first critical aggregates in the system.

The homogeneous and heterogeneous mechanisms in the global process of microcrack nucleation from dispersed vacancies are schematically illustrated in Fig. 1.

<sup>(1)</sup> In agreement with the classical nucleation theory a necessary condition for a steady state of the process to establish is that all the vacancy clusters, slightly exceeding the critical size, are removed from the system and replaced by an equivalent number of single elements. This artificial condition prevents the nuclei from unrestricted growth and gives, for each fixed strain  $\varepsilon$ , the conservation of all vacancies participating in the global process of formation of any kind of clusters within the grain. It is of no physical importance, however, since it represents only some mechanism which has to be imagined to obtain a metastable equilibrium in a supersaturated system.

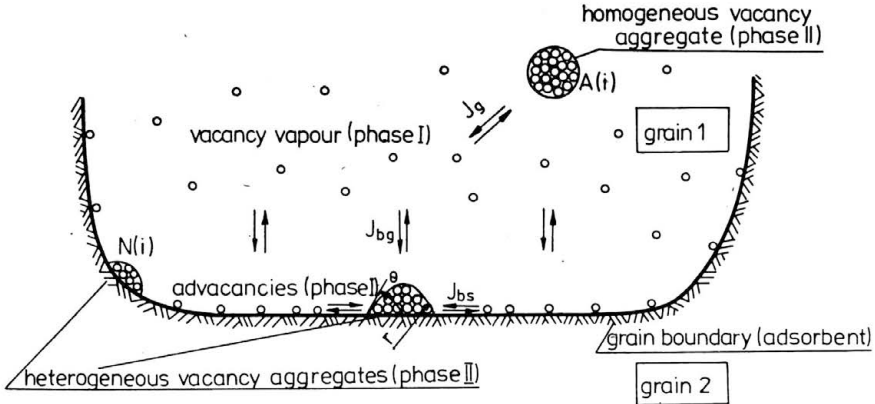


FIG. 1. Schematic model of the considered system.

Assuming that within the above mentioned time interval the nucleation process is not too rapid, so that the steady state can really be achieved, the ternary system “vacancy vapour-advacancies-vacancy aggregates” remains in a metastable equilibrium when the phase equilibria are established: vapour  $\rightleftharpoons$  homogeneous clusters, vapour + advacancies  $\rightleftharpoons$  heterogeneous clusters and an adsorption equilibrium vapour  $\rightleftharpoons$  advacancies.

### 3. Assumptions and basic preliminary formulae

Most of the assumptions concerning the adopted model of the actual body and the process considered may be summarized as follows:

- i. The crystal specimen is in a uniaxial state of strain due to tension.
- ii. The crystal has a simple cubic lattice and dislocation density negligibly small everywhere except at the grain boundaries.
- iii. Grain boundaries are free from preferential adsorption sites.
- iv. The number of all the aggregates is small compared to the total number of atomic sites and each aggregate is associated with a single site, irrespectively of its size. This concerns the grains as well as the boundaries.
- v. Only single vacancies and advacancies are mobile; the latter cannot migrate into other grains across the boundary.
- vi. It is assumed that, due to the strain, both the energies of vacancy motion and formation are lowered by the same quantity  $\Delta U(\epsilon)$  (cf. Eqs. (3.1), (3.2), (3.4)).
- vii. The clusters have spherical or hemispherical shape corresponding to the minimum of the free energy of the surface for a given volume.
- viii. Introducing formally the notion of the equilibrium contact (wetting) angle it is assumed that in the process analysed the Young's formula, joining the contact angle with appropriate surface energies, holds good.
- ix. The clusters increase or decrease in size by adding or losing one vacancy at a time. This assumption is true in the case of homogeneous clusters where one mechanism of growth is involved only, as well as in the case of heterogeneous clusters where two different mechanisms are coupled.

x. The decrease of vacancy (and advacancy) concentration around the growing aggregates and the effect of interstitials on the microcrack nucleation rate are not taken into account.

xi. Within the time period of the process observation the strain (and consequently the supersaturation of the system) increases sufficiently slowly. Thus, we can assume that after each step increase the supersaturations remain constant for times much longer than the time delay for the approach to steady state.

xii. Bulk parameters are introduced and the considerations are based on the continuum approach.

xiii. The process is considered to be isothermal ( $\text{grad } T = 0$  and  $\partial T/\partial t = 0$ ).

Below some fundamental formulas are listed. They will be used in the next sections.

Due to the strain, the activation energy of the spatial vacancy motion in the direction of the crystal elongation is reduced. The decrease of this energy ( $\Delta U$ ) was derived from simple energy considerations [6]. Subtracting the potential energy of two neighbouring lattice elements of an unstrained crystal from that of an elongated one, it was found that

$$(3.1) \quad \Delta U(\varepsilon) = aR_0^{-m} \left\{ 1 - (1 + \varepsilon)^{-m} - \frac{n}{m} [1 - (1 + \varepsilon)^{-n}] \right\},$$

where  $a$ ,  $m$ ,  $n$  are positive material constants,  $\varepsilon$  denotes the linear strain of the crystal, and  $R_0$  is the lattice constant.

The average velocity of a vacancy within the grains of the strained crystal can be approximately expressed in the form [7]

$$(3.2) \quad v = \frac{R_0}{\tau} = \nu R_0 \exp \left[ - \frac{(U_m - \Delta U)}{kT} \right],$$

where  $\tau$  is the lifetime of a vacancy at a lattice point,  $\nu \approx 10^{13} \text{ s}^{-1}$  is the atomic vibrational frequency,  $k$  is Boltzmann's constant,  $T$  is the absolute temperature, and  $U_m$  is the activation energy of motion of vacancies.

The average initial ( $\varepsilon = 0$ ) volume concentration of vacancies is given by the known formula

$$(3.3) \quad c_0 = \mathcal{N} \exp \left( - \frac{U_f}{kT} \right),$$

where  $\mathcal{N}$  is the total number of atomic sites per unit volume, and  $U_f$  is the activation energy of formation of a vacancy.

As a consequence of the crystal extension, the energy of vacancy formation is also reduced. Assuming that this energy decrease is equal to  $\Delta U$ , the actual volume vacancy concentration reads

$$(3.4) \quad c = \mathcal{N} \exp \left[ - \frac{(U_f - \Delta U)}{kT} \right] = c_0 \exp \left( \frac{\Delta U}{kT} \right).$$

It was proposed [17] that the magnitude of the formation energy decrease amounts to  $\Delta U_1 = (\varkappa \bar{\varepsilon})^2 E R_0^3$ , where  $\varkappa$  is the concentration coefficient,  $\bar{\varepsilon}$  denotes the mean linear strain, and  $E$  is Young's modulus. The quantity  $\Delta U_1$  represents the elastic energy in that volume element in which a vacancy is formed. The difference between  $\Delta U$  and  $\Delta U_1$  is,

in general, rather small. However, the use of  $\Delta U_1$  requires not only the continuum approach but also the assumption of a constitutive equation. For this reason we choose to work with  $\Delta U$  as the reduction quantity of the formation energy.

From Eq. (3.4) we obtain the ratio of the vacancy concentrations after and before the crystal is strained as a measure of the supersaturation of vacancies inside the grains

$$(3.5) \quad S_{ho} = \frac{c}{c_0} = \exp\left(\frac{\Delta U}{kT}\right).$$

From Eqs. (3.1) and (3.5) we see that for  $\varepsilon = 0$  we have  $\Delta U(\varepsilon) = 0$  as well as  $S_{ho} = 1$ .

Within the grain space the mean number of vacancies per unit time condensing on a unit area (the incidence, or capture, rate of vacancies) may be written

$$(3.6) \quad P_c = p_g cv,$$

where  $p_g$  is the probability that a vacancy will jump in the desirable direction i.e. towards an aggregate. For simple cubic lattice  $p_g$  is simply  $1/6$ , so that

$$(3.7) \quad P_c = \frac{1}{6} cv.$$

For isotropic continuum model of the crystal  $P_c$  can be evaluated in the form [3]

$$(3.8) \quad P_c = \frac{c}{\tau} \int_0^{R_0} \frac{2\pi R_0(R_0 - x)}{4\pi R_0^2} dx = \frac{1}{4} cv.$$

Here,  $1/\tau$  is the jump frequency of vacancies, and the integrand is the ratio of the surface area of a spherical segment to the surface area of the whole sphere; it represents the probability that a vacancy placed at a distance  $x$  from the aggregate surface will jump towards the aggregate. The jump distance is equal to the lattice constant  $R_0$ , and vacancies located farther than  $R_0$  have zero probability to reach the aggregate with one hop. It is clear that for continuum model of the crystal  $p_g = 1/4$ .

Substituting Eqs. (3.2) and (3.4) into Eq. (3.6) one obtains for the incidence rate the final relation

$$(3.9) \quad P_c = p_g \nu R_0 c_0 \exp\left[-\frac{(U_m - 2\Delta U)}{kT}\right].$$

A similar notion is needed to describe the heterogeneous nucleation on the grain boundary. This is the rate of impingement of advacancies on a line of unit length on the grain boundary surface (called also the capture rate). This quantity can be determined from kinetic considerations. When advacancies diffuse over the boundary with a mean velocity  $v_{sd}$ ,  $N(1)$  is the number of single advacancies per unit area of the boundary, and  $p_b$  is the probability factor that an advacancy will jump in the right direction, then

$$(3.10) \quad \omega_c = p_b N(1) v_{sd}.$$

Assuming a square lattice on the surface of the boundary  $p_b$  is simply  $1/4$ , i.e.

$$(3.11) \quad \omega_c = \frac{1}{4} N(1) v_{sd}.$$

For continuum model of the crystal  $\omega_c$  may be calculated similarly as for the three-dimensional case

$$(3.12) \quad \omega_c = \frac{N(1)}{\tau_{sd}} \int_0^d \frac{2d \arccos \frac{x}{d}}{2\pi d} dx = \frac{1}{\pi} N(1) v_{sd},$$

where  $\tau_{sd}$  is the surface diffusion lifetime of an advacancy at a lattice site ( $1/\tau_{sd}$  is the jump frequency of advacancies on the boundary surface), and the integrand is the ratio of the arc length of a circular segment to the circumference of the whole circle; it represents the probability that an advacancy located at a distance  $x$  from the periphery of the base circle of the cap-shaped aggregate will jump toward the aggregate. The jump distance is equal to the interatomic spacing  $d$  on the boundary surface, and advacancies at distances larger than  $d$  have zero probability to be incorporated into the aggregate with one hop.

The average migration velocity of a single advacancy over the grain boundary surface is approximately

$$(3.13) \quad v_{sd} = v d \exp\left(-\frac{U_{sd}}{kT}\right).$$

In the above formula the vibrational frequency, parallel to the surface, is assumed equal to that of regular atoms in the three-dimensional lattice ( $\approx 10^{13} \text{ s}^{-1}$ ),  $U_{sd}$  is the activation energy for surface autodiffusion.

Substituting Eq. (3.13) into Eq. (3.10) we obtain

$$(3.14) \quad \omega_c = p_b d v N(1) \exp\left(-\frac{U_{sd}}{kT}\right).$$

#### 4. Homogeneous nucleation of microcracks within monocrystalline grains

The process of the new phase nucleation is continuous in time and discrete in the space of natural numbers  $i$ . However, besides a discrete approach which was earlier widely used in the problem [18–20], a continuum analysis is also possible [10, 11] and will be adopted and reconsidered here. Consequently, all the functions having physical meaning only for integral values of  $i$  are formally extended onto the whole positive semi-axis. Moreover, appropriate class of each function is assumed to ensure the existence of all operations involved.

As was briefly mentioned in Sect. 2 it is always possible to define the equilibrium aggregate distribution function,  $A^0(i)$ , when there are still no perceptible traces of the new phase nuclei. This function is given, for a temperature  $T$ , by the well-known stationary Boltzmann distribution for a diluted system [2, 3, 21]

$$(4.1) \quad A^0(i) = A^0(1) \exp\left[-\frac{\Delta F_g(i) - kT \ln \frac{\mathcal{N}}{A^0(1)}}{kT}\right] = \mathcal{N} \exp\left[-\frac{\Delta F_g(i)}{kT}\right].$$

Here,  $\Delta F_g(i)$  is the free energy of formation of an aggregate of  $i$  vacancies from isolated vacancies in an isothermal reversible process ignoring the entropy of mixing; it is the sum of two terms, of which the first one is always positive and represents the work spent in forming the surface of the aggregate, and the second one is the work gained in forming the new volume. In the presence of strain, it is necessary to consider also the strain energy as part of the free energy of formation of an aggregate. Therefore, the second term should be supplemented by the total elastic potential release accompanying the creation of an element of the new phase [22, 23]. If nucleation is thermodynamically admissible ( $S_{ho} > 1$ ), the second term is always negative; otherwise, no phase transition is possible. Taking into account the minus sign for the second term, we have for spherical isotropic clusters

$$(4.2) \quad \Delta F_g(i) = 0(i)\alpha - V(i) \frac{kT}{V(1)} \ln \frac{c}{c_0} - V(i) \frac{\Delta U_1(\varepsilon)}{V(1)} \\ = 4\pi r^2 \alpha - \frac{4}{3} \pi r^3 \frac{kT}{V_v} \ln S_{ho} - \frac{4}{3} \pi r^3 \frac{\Delta U(\varepsilon)}{V_v}, \quad i \geq 2,$$

where  $0(i)$ ,  $V(i)$  and  $r = r(i)$  are surface area, volume and radius of a spherical  $i$ -mer, respectively,  $\alpha$  is the average surface tension of the crystal,  $V_v = V(1)$  is the volume of a vacancy,  $\Delta U_1(\varepsilon)$  is the decrease of the potential energy of the system connected with the formation of a unit volume of a cluster; it is assumed that  $\Delta U_1(\varepsilon) \approx \Delta U(\varepsilon)$  (cf. p. 643).

The numerator of the exponent in the first part of Eq. (4.1)

$$(4.3) \quad \tilde{\Delta F}_g(i) = \Delta F_g(i) - kT \ln \frac{\mathcal{N}}{A^0(1)},$$

presents the cluster formation energy completed with the configurational entropy term  $-kT \ln(\mathcal{N}/A^0(1))$  [24], under the assumption that  $\mathcal{N} \gg \Sigma A^0(i)$  i.e. that the number of all the aggregates is small compared with the total number of atomic sites. Since no energy is needed to form an aggregate of one vacancy from single vacancies the total free energy of formation  $\tilde{\Delta F}_g$  should be zero for  $i = 1$ . Thus

$$(4.4) \quad \tilde{\Delta F}_g(1) = \Delta F_g(1) - kT \ln \frac{\mathcal{N}}{A^0(1)} = 0,$$

and we have

$$(4.5) \quad \Delta F_g(1) = U_f = kT \ln \frac{\mathcal{N}}{A^0(1)}.$$

Because  $A^0(1) = c_0$ , this is in accordance with Eq. (3.3).

From Eqs. (4.3) and (4.5) it follows that

$$(4.6) \quad \tilde{\Delta F}_g(i) = \Delta F_g(i) - \Delta F_g(1).$$

Utilizing the relations

$$(4.7) \quad i = \frac{V(i)}{V(1)} = \frac{4\pi r^3}{3V_v}, \quad 0(i) = (36\pi)^{1/3} V_v^{2/3} i^{2/3},$$

we can express  $\Delta F_g$  as a function of the variable  $i$

$$(4.8) \quad \Delta F_g(i) = \begin{cases} (36\pi)^{1/3} V_v^{2/3} \alpha i^{2/3} - i[kT \ln S_{ho} + \Delta U(\varepsilon)] & \text{for } i \geq 2, \\ kT \ln \frac{\mathcal{N}}{c_0} & \text{for } i = 1. \end{cases}$$



When  $S_{ho} > 1$  the first derivative of  $\Delta F_g(i)$  equals zero

$$(4.9) \quad \frac{\partial \Delta F_g(i)}{\partial i} = \frac{2}{3} (36\pi)^{1/3} V_v^{2/3} \alpha i^{-1/3} - (kT \ln S_{ho} + \Delta U) = 0,$$

at a point  $i = i_g^*$

$$(4.10) \quad i_g^* = \frac{32\pi\alpha^3 V_v^2}{3(kT \ln S_{ho} + \Delta U)^3} = \frac{4\pi\alpha^3 V_v^2}{3[\Delta U(\epsilon)]^3},$$

where the supersaturation  $S_{ho}$  is expressed by  $\Delta U(\epsilon)$ , according to Eq. (3.5).

Since the second derivative of  $\Delta F_g(i)$  is negative at that point

$$(4.11) \quad \left[ \frac{\partial^2 \Delta F_g(i)}{\partial i^2} \right]_{i=i_g^*} = -\frac{2}{9} (36\pi)^{1/3} V_v^{2/3} \alpha i_g^{*-4/3} < 0,$$

the function  $\Delta F_g$  reaches a maximum at the critical cluster of  $i_g^*$  vacancies

$$(4.12) \quad \Delta F_g(i_g^*) = \Delta F_g^* = \frac{16\pi\alpha^3 V_v^2}{3(kT \ln S_{ho} + \Delta U)^2} = \frac{4\pi\alpha^3 V_v^2}{3[\Delta U(\epsilon)]^2}.$$

Let us now consider an arbitrary internal subregion of a grain (cf. Fig. 1) of the crystal sample subject to uniaxial strain. When, under the increasing strain, the supersaturation of vacancies in the considered system attains a sufficiently high value a certain number of critical aggregates (microcrack nuclei) is formed. Let the number of nuclei formed per unit volume and unit time, at a given temperature  $T$  and strain  $\epsilon$ , be  $J_g(i, t)$ . It is called the homogeneous nucleation rate, and results from a flux which flows through all the aggregate classes from smaller to larger aggregates. Its intensity is equal to the difference between the numbers of aggregates that pass to the next higher class by addition of single vacancies and those that return to the lower class by separation of single vacancies. The nucleation rate  $J_g(i, t)$  can, therefore, be written

$$(4.13) \quad J_g(i, t) = A(i-1, t) P_c 0(i-1) - A(i, t) P_e(i) 0(i), \quad i \geq 2,$$

where  $A(i, t)$  is the non-equilibrium density of aggregates of  $i$  vacancies at a time  $t$ , and  $P_e(i)$  is the emission rate of vacancies per unit area of the surface of an aggregate of size  $i$ .

Under equilibrium conditions there is no phase transition and the net flow of aggregates must vanish. Consequently,  $A(i, t) = A^0(i)$  and we get

$$(4.14) \quad J_g(i, t) = A^0(i-1) P_c 0(i-1) - A^0(i) P_e(i) 0(i) = 0.$$

Since the mechanism of growth and decay of the aggregates should not be affected by the fact whether or not the system is in equilibrium, the functions  $P_c$  and  $P_e(i)$  should be of the same form under all conditions [21, 25]. Thus, from Eq. (4.14) we can find  $P_e(i)$  as a function of  $P_c$

$$(4.15) \quad P_e(i) = \frac{A^0(i-1) 0(i-1)}{A^0(i) 0(i)} P_c.$$

Introduction of Eq. (4.15) into Eq. (4.13) yields

$$(4.16) \quad J_g(i, t) = P_c 0(i-1) \left[ A(i-1, t) - A(i, t) \frac{A^0(i-1)}{A^0(i)} \right].$$

Now, in Eq. (4.16) we assume that  $0(i-1) \approx 0(i)$ , and we expand the functions  $A(i-1, t)$  and  $A^0(i-1)$  into Taylor series near the point  $i$ , linearizing the expansions. This leads to

$$(4.17) \quad J_g(i, t) = P_c 0(i) \left[ \frac{A(i, t)}{A^0(i)} \frac{\partial A^0(i)}{\partial i} - \frac{\partial A(i, t)}{\partial i} \right].$$

If one neglects small values of the argument  $i$ , all the functions appearing in Eq. (4.16) show only a very slight change as  $i$  varies by one unit. Hence, the above approximations are acceptable for all but small aggregates, the more so that we are mainly interested in variations of the functions near the point  $i = i_g^*$ , and that the effect of the values of all the functions for small  $i$  on the nucleation rate is rather minute [8].

Differentiating the function (4.1)

$$(4.18) \quad \frac{\partial A^0(i)}{\partial i} = - \frac{A^0(i)}{kT} \frac{\partial \Delta F_g(i)}{\partial i},$$

and substituting the result into Eq. (4.17) we find

$$(4.19) \quad J_g(i, t) = -P_c 0(i) \left[ \frac{A(i, t)}{kT} \frac{\partial \Delta F_g(i)}{\partial i} + \frac{\partial A(i, t)}{\partial i} \right].$$

The functions  $A(i, t)$  and  $J_g(i, t)$  must satisfy, for each  $\varepsilon$ , the equation of continuity which for the considered sourceless process is reduced to the form

$$(4.20) \quad \frac{\partial A(i, t)}{\partial t} + \frac{\partial J_g(i, t)}{\partial i} = 0.$$

Inserting the flux, Eq. (4.19), into Eq. (4.20) we obtain

$$(4.21) \quad \frac{\partial A(i, t)}{\partial t} - P_c \frac{\partial}{\partial i} \left\{ 0(i) \left[ \frac{A(i, t)}{kT} \frac{\partial \Delta F_g(i)}{\partial i} + \frac{\partial A(i, t)}{\partial i} \right] \right\} = 0.$$

Assuming that the process achieves a steady state (the time delay to attain this steady state is usually negligibly short [3, 26, 27]), we put  $\partial A(i, t)/\partial t = 0$  in Eq. (4.21), and the problem is reduced to the following linear differential equation for the distribution function  $A(i)$ , which now is independent of time,

$$(4.22) \quad 0(i) \frac{\partial A(i)}{\partial i} + \frac{0(i)}{kT} \frac{\partial \Delta F_g(i)}{\partial i} A(i) = C,$$

where  $C$  is a constant.

Equation (4.22) can also be obtained by stating that in the steady state the intensity of the flux of aggregates is constant i.e. by putting  $J_g(i, t) = \text{const}$  in Eq. (4.19).

The general solution of Eq. (4.22) reads

$$(4.23) \quad A(i) = \exp \left[ \frac{\Delta F_g(1) - \Delta F_g(i)}{kT} \right] \left\{ C_1 + C \exp \left[ - \frac{\Delta F_g(1)}{kT} \right] \right. \\ \left. \times \int_0^i \frac{1}{0(i)} \exp \left[ \frac{\Delta F_g(i)}{kT} \right] di \right\},$$

where  $C_1$  is a constant, and  $\Delta F_g(1)$  is given by Eq. (4.5). We then set the boundary conditions for the function  $A(i)$ :

$$(4.24) \quad \begin{aligned} 1. \quad & \text{For } i = 1, \quad A(1) = c \text{—the actual vacancy concentration,} \\ 2. \quad & \text{For } i = \infty, \quad \lim_{i \rightarrow \infty} A(i) = 0. \end{aligned}$$

Taking into account the following limit

$$\lim_{i \rightarrow \infty} \frac{\Delta F_g(i)}{kT} = -\infty,$$

the conditions (4.24)<sub>1,2</sub> imposed on the function (4.23) allow to specify the constants  $C$  and  $C_1$  and lead to the particular solution of Eq. (4.22) for the non-equilibrium stationary distribution of aggregates

$$(4.25) \quad A(i) = \mathcal{N} S_{ho} \exp \left[ -\frac{\Delta F_g(i)}{kT} \right] \left\{ 1 - \frac{\int_1^i \frac{1}{0(i)} \exp \left[ \frac{\Delta F_g(i)}{kT} \right] di}{\int_1^\infty \frac{1}{0(i)} \exp \left[ \frac{\Delta F_g(i)}{kT} \right] di} \right\}.$$

Substituting Eq. (4.25) into the flux equation (4.19) we determine the steady state nucleation rate

$$(4.26) \quad J_g(i, t) = J_g = \frac{P_c \mathcal{N} S_{ho}}{\int_1^\infty [0(i)]^{-1} \exp \left[ \frac{\Delta F_g(i)}{kT} \right] di} = \text{const.}$$

To estimate the integral in the denominator of Eqs. (4.25) and (4.26) we follow a simplification suggested by FRENKEL [21]. We namely expand the function  $\Delta F_g(i)$  into Taylor series at the point of its maximum  $i_g^*$ , neglecting all the terms above the third one, i.e.

$$(4.27) \quad \Delta F_g(i) \approx \Delta F_g^* + \left[ \frac{\partial \Delta F_g(i)}{\partial i} \right]_{i_g^*} (i - i_g^*) + \frac{1}{2} \left[ \frac{\partial^2 \Delta F_g(i)}{\partial i^2} \right]_{i_g^*} (i - i_g^*)^2.$$

Taking advantage of Eqs. (4.9), (4.10) and (4.11) and replacing  $0(i)$ , given by Eq. (4.7)<sub>2</sub>, by its value for  $i = i_g^*$  (in view of a very sharp maximum of the integrand  $\exp[\Delta F_g(i)/kT]$  at this point), we get an integral related to the Gauss probability integral which can be simply evaluated to give

$$(4.28) \quad \int_1^\infty [0(i)]^{-1} \exp \left[ \frac{\Delta F_g(i)}{kT} \right] di \approx \frac{1}{2V_v} \sqrt{\frac{kT}{\alpha}} \exp \left( \frac{\Delta F_g^*}{kT} \right).$$

Substituting the integral (4.28) into Eq. (4.26) we obtain the final form of the homogeneous steady state nucleation rate of vacancy-microcracks within monocrystalline grains of the strained crystal

$$(4.29) \quad J_g = 2 \mathcal{N} S_{ho} P_c V_v \sqrt{\frac{\alpha}{kT}} \exp \left( -\frac{\Delta F_g^*}{kT} \right).$$

Coming back to the non-equilibrium distribution of vacancy clusters we insert the integral (4.28) into (4.25) arriving at the final expression for  $A(i)$

$$(4.30) \quad A(i) = \mathcal{N} S_{\text{ho}} \exp \left[ -\frac{\Delta F_g(i)}{kT} \right] \left\{ 1 - 2V_v \sqrt{\frac{\alpha}{kT}} \exp \left( -\frac{\Delta F_g^*}{kT} \right) \times \int_1^i \frac{1}{0(i)} \exp \left[ \frac{\Delta F_g(i)}{kT} \right] di \right\}.$$

Since the entropy of mixing and the release of the strain energy are included in the total formation energy of an aggregate  $\tilde{\Delta F}_g(i)$ , Eqs. (4.29) and (4.30) differ in the preexponential factor from the analogical equations derived earlier [6, 8, 10].

The same approximate procedure can be also applied [28] to the last integral in Eq. (4.30), under the condition that its upper integration limit lies close enough to the point  $i_g^*$ , so that the integral may be determined mainly by the left-sided part of the maximum of  $\exp[\Delta F_g(i)/kT]$ . In particular, for  $i = i_g^*$  we get in the same way

$$(4.31) \quad \int_1^{i_g^*} [0(i)]^{-1} \exp \left[ -\frac{\Delta F_g(i)}{kT} \right] di \approx \frac{1}{4V_v} \sqrt{\frac{kT}{\alpha}} \exp \left( \frac{\Delta F_g^*}{kT} \right).$$

and

$$(4.32) \quad A(i_g^*) = \frac{1}{2} \mathcal{N} S_{\text{ho}} \exp \left( -\frac{\Delta F_g^*}{kT} \right) = \frac{1}{2} S_{\text{ho}} A^0(i_g^*).$$

It is worth noting that further analysis of the distribution function  $A(i)$  shows, in contradistinction to  $A^0(i)$ , that it does not reach a minimum but decreases asymptotically to zero with increasing  $i$ . This is in accordance with the condition (4.24)<sub>2</sub>.

The appearance of the three-dimensional flux of vacancies in the homogeneous as well as in the heterogeneous nucleation kinetics makes both the processes coupled rather than linearly superposed. However, rough quantitative estimates show that the effect of coupling on the homogeneous nucleation mechanism is very small, and has been neglected here. It is taken into consideration in the heterogeneous nucleation (Sect. 7).

## 5. Heterogeneous microcrack nucleation due to the sole addition of vacancies from the grain space

In Sect. 4 the conditions of formation of the homogeneous microcrack nuclei in single crystals were investigated. They concerned either artificially grown nearly perfect crystals (whiskers) or internal monocrystalline spaces of the grains of a polycrystal. The former are free from dislocations and other imperfections of a real crystalline structure, frequently to a very high degree, and the theory applies to them fairly well. To the latter, however, the classical nucleation theory can be applied only in a more approximate manner.

The aim of this, and the following sections, is to extend the theory to polycrystalline materials by considering also the effect of intercrystalline boundaries on the process of microcrack generation. It is known that the vacancy agglomerations are formed much

more easily on the grain boundaries than within the grains. Thus one of the ways which can bring us closer to the early stage of real microfracture mechanism consists in examining the process of nonhomogeneous nucleation of microcracks from dispersed vacancies.

Beside the homogeneous clusters formed within the grains of the strained crystal, heterogeneous vacancy aggregations in the shape of spherical segments are originated at the grain boundaries. Two mechanisms are involved in the formation of each heterogeneous cluster: direct impingement of single vacancies from the grain on the surface of the cluster, and joining of separate advacancies to the periphery of the cluster due to the surface diffusion. Both mechanisms are coupled. However, in this section and the next one we will treat them formally as uncoupled assuming, in the first place, that the process involving addition of vacancies from the grain space is the only active mechanism.

Let us fix our attention on a segment of the grain boundary transverse to the direction of the crystal elongation. We assume that the cap-shaped vacancy islands lie on a two-dimensional square lattice of lattice parameter  $d$ , and that the equilibrium distribution of aggregate sizes  $N^0(i)$  is determined, for a given temperature  $T$ , by the formula

$$(5.1) \quad N^0(i) = N^0(1) \exp \left[ - \frac{\Delta F_{bg}(i) - kT \ln \frac{N_0}{N^0(1)}}{kT} \right] = N_0 \exp \left[ - \frac{\Delta F_{bg}(i)}{kT} \right].$$

Here,  $N_0$  is the density of discrete adsorption sites per unit area of the grain boundary ( $N_0 \approx 1/d^2 \approx 10^{15} \text{ cm}^{-2}$ ), the mixing entropy term  $-kT \ln(N_0/N^0(1))$  [29] is included and it is assumed that  $N_0 \gg N^0(1) \approx \sum N^0(i)$ , which means that the fraction of the unit area of the grain boundary surface covered by the aggregates of various classes is negligibly small;  $\Delta F_{bg}(i)$  is the free energy of formation of a single cluster of  $i$  vacancies in an isolated reversible process involving solely the growth of the cluster by acquisition of vacancies from the grain space (the curvature effect), and with the configurational entropy disregarded.  $\Delta F_{bg}(i)$  is postulated in the form

$$(5.2) \quad \Delta F_{bg}(i) = W(i) - \frac{\bar{V}(i)}{V_v} \left[ kT \ln \frac{c}{c_0} + \Delta U(\varepsilon) \right], \quad i \geq 2,$$

where  $W(i)$  is the work spent in forming the surface of the cluster, and the second term represents the work gained in forming the new volume in the presence of strain [22];  $\bar{V}(i)$  is the volume of an  $i$ -mer of the shape of a spherical segment.

The total free energy of formation, appearing in the exponent of the first part of Eq. (5.1),

$$(5.3) \quad \tilde{\Delta F}_{bg}(i) = \Delta F_{bg}(i) - kT \ln \frac{N_0}{N^0(1)},$$

should vanish for  $i = 1$ . Consequently, it follows that

$$(5.4) \quad \Delta F_{bg}(1) = kT \ln \frac{N_0}{N^0(1)},$$

and

$$(5.5) \quad \tilde{\Delta F}_{bg}(i) = \Delta F_{bg}(i) - \Delta F_{bg}(1).$$

Taking advantage of the geometry of the aggregate and introducing formally the notion of the equilibrium contact angle  $\theta$ , which makes the aggregate with the grain boundary (Fig. 1), we can evaluate the first term in Eq. (5.2). To this end we accept the Young's formula in which  $\theta$  is determined by the relevant specific interfacial free energies at adjacent surfaces

$$(5.6) \quad \alpha_{bg} = \alpha_{ba} + \alpha \cos \theta,$$

where the subscripts  $b$ ,  $g$ , and  $a$  refer to the grain boundary, grain space and the aggregate, respectively, and  $\alpha$  is the surface free energy of the crystal.

If  $S(i)$  and  $S'(i)$  denote the surface area of the cap of the aggregate and the area of its base, and  $r$  is the radius of curvature of the aggregate, we can write, using Eq. (5.6)

$$(5.7) \quad W(i) = S(i)\alpha + S'(i)(\alpha_{ba} - \alpha_{bg}) = 4\pi r^2 \alpha \Phi(\theta),$$

where

$$(5.8) \quad \Phi(\theta) = \frac{1}{4}(2 - 3\cos\theta + \cos^3\theta),$$

is the ratio of the volume of a spherical segment to the volume of the entire sphere.

Making use of the relation

$$(5.9) \quad i = \frac{\bar{V}(i)}{V_v} = \frac{4\pi r^3}{3V_v} \Phi(\theta),$$

in Eqs. (5.7) and (5.2), we obtain  $\Delta F_{bg}$  as a function of  $i$

$$(5.10) \quad \Delta F_{bg}(i) = \begin{cases} (36\pi)^{1/3} V_v^{2/3} \Phi^{1/3} \alpha i^{2/3} - i[kT \ln S_{ho} + \Delta U(\varepsilon)] & \text{for } i \geq 2, \\ kT \ln \frac{N_0}{N^0(1)} & \text{for } i = 1. \end{cases}$$

It is worth noting that for  $i \geq 2$ ,  $\Delta F_{bg}(i)$  differs from  $\Delta F_g(i)$  in the first term only (cf. Eq. (4.8)<sub>1</sub>), in view of the change of the cluster shape.

For supersaturation  $S_{ho} > 1$  we have

$$(5.11) \quad \frac{\partial \Delta F_{bg}(i)}{\partial i} = \frac{2}{3} (36\pi)^{1/3} V_v^{2/3} \Phi^{1/3} \alpha i^{1/3} - (kT \ln S_{ho} + \Delta U) = 0,$$

at a point

$$(5.12) \quad i_{bg}^* = \frac{32\pi\alpha^3 V_v^2}{3(kT \ln S_{ho} + \Delta U)^3} \Phi = \frac{4\pi\alpha^3 V_v^2}{3[\Delta U(\varepsilon)]^3} \Phi.$$

Since

$$(5.13) \quad \left[ \frac{\partial^2 \Delta F_{bg}(i)}{\partial i^2} \right]_{i=i_{bg}^*} = -\frac{2}{9} (36\pi)^{1/3} V_v^{2/3} \Phi^{1/3} \alpha i_{bg}^{*-4/3} < 0,$$

$\Delta F_{bg}(i)$  exhibits a maximum at the critical aggregate consisting of  $i_{bg}^*$  vacancies

$$(5.14) \quad \Delta F_{bg}(i_{bg}^*) = \Delta F_{bg}^* = \frac{16\pi\alpha^3 V_v^2}{3(kT \ln S_{ho} + \Delta U)^2} \Phi = \frac{4\pi\alpha^3 V_v^2}{3[\Delta U(\varepsilon)]^2} \Phi.$$

The range of the contact angle function  $\Phi(\theta)$  is the interval  $\langle 0, 1 \rangle$  when  $\theta$  varies from 0 to  $\pi$  (cf. Eq. (5.8)). For  $\theta = 0, \Phi(\theta) = 0$  and  $\Delta F_{bg}^* = 0$ , and nucleation will be most

rapid (complete condensation). For  $\theta = \pi$ ,  $\Phi(\theta) = 1$  and  $\Delta F_{bg}^* = \Delta F_g^*$  so that the nucleus will have the spherical shape and homogeneous nucleation takes place. This is the limiting case in which the grain boundary has no catalytic effect on the nucleation process, and the nuclei are formed with the same rate within the grain as well as on the grain boundary.

Moreover, we note that

$$(5.15) \quad i_{bg}^* = i_g^* \Phi \quad \text{and} \quad \Delta F_{bg}^* = \Delta F_g^* \Phi$$

so that

$$(5.16) \quad i_{bg}^* \leq i_g^* \quad \text{and} \quad \Delta F_{bg}^* \leq \Delta F_g^*$$

for the same  $\varepsilon$  and  $T$ . Since in this case the energy barrier to nucleation  $\Delta F_{bg}^*$  is lower than  $\Delta F_g^*$ , heterogeneous nucleation due to the surface addition of vacancies from the grain space proceeds always faster than the homogeneous one (cf. Tables 2, 3 and 4 in Sect. 10).

Similarly as in the homogeneous case we consider now the net flow of heterogeneous void embryos, denoting it by  $J_{bg}(i, t)$ . Since the growth process is limited to the sole addition of vacancies from the grain space, the nucleation rate equation reads

$$(5.17) \quad J_{bg}(i, t) = N(i-1, t)P_c S(i-1) - N(i, t)P_e(i)S(i), \quad i \geq 2,$$

where  $N(i, t)$  is the non-equilibrium surface density of heterogeneous clusters of size  $i$  at a time  $t$ ,  $P_c$  and  $P_e(i)$  retain their previous meanings, and  $S(i)$  being the surface area of the cluster cap is, according to Eq. (5.9), given by the relation

$$(5.18) \quad S(i) = 2\pi r^2(1 - \cos \theta) = \left(\frac{9\pi}{2}\right)^{1/3} V_v^{2/3} \Phi^{-2/3} (1 - \cos \theta) i^{2/3}.$$

If the system is in a state of equilibrium there is no nucleation so that  $J_{bg}(i, t) = 0$  and  $N(i, t) = N^0(i)$  in Eq. (5.17). This enables us to eliminate  $P_e(i)$  from Eq. (5.17). Next, the functions  $N(i-1, t)$  and  $N^0(i-1)$  are expanded into Taylor series in the neighbourhood of the point  $i$ , and all the terms above the second one are disregarded. Moreover, we put  $S(i-1) \approx S(i)$ , and after differentiating the function (5.1) we substitute the derivative  $\partial N^0(i)/\partial i$  into the transformed flux equation, getting

$$(5.19) \quad J_{bg}(i, t) = -P_c S(i) \left[ \frac{N(i, t)}{kT} \frac{\partial \Delta F_{bg}(i)}{\partial i} + \frac{\partial N(i, t)}{\partial i} \right].$$

By substituting Eq. (5.19) into the equation of continuity ( $\partial N/\partial t + \partial J_{bg}/\partial i = 0$ ), and assuming that a steady state is attained i.e.  $\partial N(i, t)/\partial t = 0$  (or  $J_{bg}(i, t) = \text{const}$ ), we obtain a linear differential equation for the cluster distribution function  $N(i)$

$$(5.20) \quad S(i) \frac{\partial N(i)}{\partial i} + \frac{S(i)}{kT} \frac{\partial \Delta F_{bg}(i)}{\partial i} N(i) = C,$$

where  $C$  is a constant.

Setting the boundary conditions:  $N(1) = \text{constant}$ ,  $N(\infty) = 0$  we finally obtain the particular solution of Eq. (5.20) in the form

$$(5.21) \quad N(i) = N_0 S_{\text{het}} \exp \left[ -\frac{\Delta F_{bg}(i)}{kT} \right] \left\{ 1 - \frac{\int_1^i \frac{1}{S(i)} \exp \left[ \frac{\Delta F_{bg}(i)}{kT} \right] di}{\int_1^\infty \frac{1}{S(i)} \exp \left[ \frac{\Delta F_{bg}(i)}{kT} \right] di} \right\},$$

where

$$(5.22) \quad S_{\text{het}} = \frac{N(1)}{N^0(1)}$$

is defined as the supersaturation of advacancies at the grain boundaries ( $S_{\text{het}}$  is calculated in Sect. 6, cf. Eq. (6.5)).

By inserting Eq. (5.21) into Eq. (5.19) we arrive at the steady state nucleation rate

$$(5.23) \quad J_{bg}(i, t) = J_{bg} = \frac{N_0 S_{\text{het}} P_c}{\int_1^\infty [S(i)]^{-1} \exp \left[ \frac{\Delta F_{bg}(i)}{kT} \right] di} = \text{const.}$$

In Eq. (5.23) we now replace  $S(i)$ , given by Eq. (5.18), by  $S(i_{bg}^*)$  and we expand the function  $\Delta F_{bg}(i)$  into power series about  $i_{bg}^*$  keeping terms to the second order and making use of Eqs. (5.11), (5.12) and (5.13). Performing these approximations in the same manner as in Sect. 4, the integral in Eq. (5.23) can be easily calculated to yield

$$(5.24) \quad \int_1^\infty [S(i)]^{-1} \exp \left[ \frac{\Delta F_{bg}(i)}{kT} \right] di \approx \frac{1}{V_v} \sqrt{\frac{kT}{\alpha}} \frac{\Phi^{1/2}}{1 - \cos \theta} \exp \left( \frac{\Delta F_{bg}^*}{kT} \right),$$

so that after coming back to Eq. (5.23) the isolated heterogeneous cap surface-growth-controlled nucleation rate of microcracks on the grain boundaries reads

$$(5.25) \quad J_{bg} = N_0 S_{\text{het}} P_c V_v \sqrt{\frac{\alpha}{kT\Phi}} (1 - \cos \theta) \exp \left( -\frac{\Delta F_{bg}^*}{kT} \right).$$

Introduction of the integral (5.24) into Eq. (5.21) delivers the final expression for the non-equilibrium distribution function  $N(i)$

$$(5.26) \quad N(i) = N_0 S_{\text{het}} \exp \left[ -\frac{\Delta F_{bg}(i)}{kT} \right] \left\{ 1 - V_v \sqrt{\frac{\alpha}{kT\Phi}} (1 - \cos \theta) \times \exp \left( -\frac{\Delta F_{bg}^*}{kT} \right) \int_1^i \frac{1}{S(i)} \exp \left[ \frac{\Delta F_{bg}(i)}{kT} \right] di \right\}.$$

A similar approximate procedure may also be applied to the integral in Eq. (5.26).

## 6. Heterogeneous nucleation by the isolated surface diffusion mechanism

Consider again a segment of the grain boundary perpendicular to the direction of the crystal elongation. We assume now that the problem of heterogeneous nucleation of vacancy microcracks at the boundary is uncoupled and depends only on the surface diffusion mechanism.



Under the conditions of adsorption equilibrium at the grain boundary surface the incidence flux of vacancies will equal the desorption flux. This can be written approximately

$$(6.1) \quad P_c(1-f_b) = \frac{N(1)}{\tau_{des}}(1-f_g),$$

where  $f_b = N(1)/N_0$  so that  $(1-f_b)$  is the fraction of a unit area of the boundary surface not occupied by advacancies,  $f_g = c/\mathcal{N}$  is the fractional concentration of vacancies within the grain,

$$(6.2) \quad \tau_{des} = \frac{1}{\nu} \exp\left(\frac{U_{des} - \Delta U}{kT}\right)$$

is the mean lifetime of an advacancy on the grain boundary before desorption, and  $U_{des}$  is the activation energy for desorption of an advacancy from the grain boundary surface which is also reduced by  $\Delta U(\varepsilon)$ , similarly as in the case of the activation energy of vacancy motion.

$U_{des}$  is connected with the activation energy for adsorption,  $U_{ad} = U_m$ , through the heat of adsorption  $E_a$  (Fig. 2)

$$(6.3) \quad E_a = U_{des} - U_m,$$

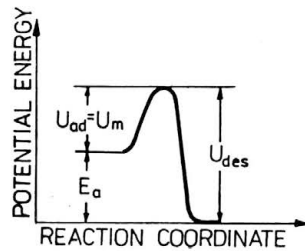


FIG. 2. Variation of potential energy accompanying adsorption and desorption, and the interrelation between  $E_a$ ,  $U_{ad}$  and  $U_{des}$ .

Solving Eq. (6.1) for  $N(1)$  we obtain

$$(6.4) \quad N(1) = \frac{P_c}{\frac{1}{\tau_{des}} \left(1 - \frac{c}{\mathcal{N}}\right) + \frac{P_c}{N_0}}.$$

It should be mentioned that in Eq. (6.4) the consumption of advacancies for heterotogeneous nucleation is disregarded (cf. assumption x, in Sect. 3). This rather small effect is taken into consideration in ref. [16].

The surface supersaturation of advacancies for the heterogeneous process was defined in Sect. 5 (Eq. (5.22)) as the ratio  $S_{het} = N(1)/N^0(1)$ . Consequently, writing Eq. (6.4) for the actual state ( $\varepsilon > 0$ ) and for the initial one ( $\varepsilon = 0$ ), and using Eqs. (3.5), (3.9), (6.2) and (6.3), we find

$$(6.5) \quad S_{het} = \frac{N(1)}{N^0(1)} = S_{ho}H(\varepsilon),$$

where

$$(6.6) \quad H(\varepsilon) = \frac{\exp\left(-\frac{E_a}{kT}\right)(\mathcal{N} - c_0) + \frac{p_g \mathcal{N} R_0}{N_0} c_0}{\exp\left(-\frac{E_a}{kT}\right)(\mathcal{N} - c) + \frac{p_g \mathcal{N} R_0}{N_0} c}$$

We notice that  $H(\varepsilon)$  is within the interval  $(0,1)$  and that for  $\varepsilon = 0$ ,  $\Delta U(\varepsilon) = 0$  and  $c = c_0$  so that  $H(\varepsilon) = 1$  and  $S_{het} = S_{no} = 1$ .

In order to determine the final form of the impingement rate of advacancies on a line of unit length on the boundary surface ( $\omega_c$ ), we substitute  $N(1)$  from Eq. (6.4) into Eq. (3.14) getting

$$(6.7) \quad \omega_c = \frac{p_b p_g \nu R_0 \mathcal{N} c_0 d}{\left[\exp\left(-\frac{E_a}{kT}\right)(\mathcal{N} - c) + \frac{p_g \mathcal{N} R_0}{N_0} c\right]} \exp\left(\frac{\Delta U - U_{sd}}{kT}\right).$$

The equilibrium distribution of vacancy clusters  $N^0(i)$  is now assumed in the form

$$(6.8) \quad N^0(i) = N^0(1) \exp\left[-\frac{\Delta F_{bs}(i) - kT \ln \frac{N_0}{N^0(1)}}{kT}\right] = N_0 \exp\left[-\frac{\Delta F_{bs}(i)}{kT}\right],$$

where the sum  $\tilde{\Delta F}_{bs}(i) = \Delta F_{bs}(i) - kT \ln(N_0/N^0(1))$  is the total energy of formation of a cluster composed of  $i$  advacancies in a process involving only the surface diffusion mechanism;  $\Delta F_{bs}(i)$  is a size-dependent term, and  $-kT \ln(N_0/N^0(1))$  [29] is the correction for the free energy of distributing the clusters on the  $N_0$  available adsorption sites (configurational entropy term). Since  $\tilde{\Delta F}_{bs}(1)$  must be zero,  $\Delta F_{bs}(1) = kT \ln(N_0/N^0(1))$ , and for cap-shaped clusters the size-dependent term  $\Delta F_{bs}(i)$  in the presence of strain can be postulated in the form

$$(6.9) \quad \Delta F_{bs}(i) = \begin{cases} (36\pi)^{1/3} V_v^{2/3} \Phi^{1/3} \alpha i^{2/3} - i[kT \ln S_{het} + \Delta U(\varepsilon)] & \text{for } i \geq 2 \\ kT \ln \frac{N_0}{N^0(1)} & \text{for } i = 1. \end{cases}$$

Because the growth of clusters is governed now by the surface supersaturation  $S_{het}$  we see that for  $i \geq 2$ ,  $\Delta F_{bs}(i)$  differs from  $\Delta F_{bg}(i)$  in the second term (cf. Eq. (5.10)<sub>1</sub>).

Similarly as  $\Delta F_g$  and  $\Delta F_{bg}$  the function  $\Delta F_{bs}$  has a maximum

$$(6.10) \quad \Delta F_{bs}(i_{bs}^*) = \Delta F_{bs}^* = \frac{16\pi\alpha^3 V_v^2}{3(kT \ln S_{het} + \Delta U)^2} \Phi = \frac{16\pi\alpha^3 V_v^2}{3[2\Delta U(\varepsilon) + kT \ln H(\varepsilon)]^2} \Phi$$

at the critical cluster size

$$(6.11) \quad i_{bs}^* = \frac{32\pi\alpha^3 V_v^2}{3(kT \ln S_{het} + \Delta U)^3} \Phi = \frac{32\pi\alpha^3 V_v^2}{3[2\Delta U(\varepsilon) + kT \ln H(\varepsilon)]^3} \Phi.$$

Comparing Eqs. (5.12) and (6.11) as well as Eqs. (5.14) and (6.10) we notice that

$$(6.12) \quad i_{bg}^* = i_{bs}^* \left(\frac{2\Delta U + kT \ln H}{2\Delta U}\right)^3 \quad \text{and} \quad \Delta F_{bg}^* = \Delta F_{bs}^* \left(\frac{2\Delta U + kT \ln H}{2\Delta U}\right)^2.$$

Since  $0 < H \leq 1$  and  $i_{bg}^*$  must be non-negative,  $-2\Delta U \leq kT \ln H \leq 0$  so that  $(2\Delta U + kT \ln H)/2\Delta U \in \langle 0, 1 \rangle$  and we have

$$(6.13) \quad i_{bg}^* \leq i_{bs}^* \quad \text{and} \quad \Delta F_{bg}^* \leq \Delta F_{bs}^*$$

for the same  $\varepsilon$  and  $T$ . Although in this case the energy barrier to nucleation  $\Delta F_{bs}^*$  is higher than  $\Delta F_{bg}^*$ , heterogeneous nucleation by the isolated surface diffusion mechanism,  $J_{bs}$ , proceeds in general faster than the heterogeneous nucleation process  $J_{bg}$  (cf. Table 6 in Sect. 10). The reason for this is that, on the one hand, the differences between  $\Delta F_{bg}^*$  and  $\Delta F_{bs}^*$  are rather small (the coefficient  $(2\Delta U + kT \ln H)/2\Delta U$  is, in general, close to unity) and, on the other hand, the remaining factors appearing in  $J_{bs}$  significantly increase this rate in comparison with  $J_{bg}$  (cf. Eqs. (5.25) and (6.18)).

Passing now to the kinetics we denote here the isolated flux of clusters by  $J_{bs}(i, t)$ . Since in this case the growth mechanism is controlled only by the surface diffusion of advacancies, the nucleation rate equation reads

$$(6.14) \quad J_{bs}(i, t) = N(i-1, t)\omega_c l(i-1) - N(i, t)\omega_e(i)l(i), \quad i \geq 2,$$

where  $\omega_e(i)$  is the emission rate of advacancies from the unit length of the periphery of the base of a cap-shaped  $i$ -mer, and  $l(i)$  is the length of this periphery which, by using the relation (5.9), can be expressed as

$$(6.15) \quad l(i) = 2\pi r \sin \theta = (6\pi^2)^{1/3} V_v^{1/3} \Phi^{-1/3} \sin \theta i^{1/3}.$$

We now follow again the lines of Sect. 5, bearing in mind that here instead of  $S(i)$ ,  $P_c$ , and  $\Delta F_{bg}(i)$  we have to use the quantities  $l(i)$ ,  $\omega_c$  and  $\Delta F_{bs}(i)$ , respectively. Consequently, we first eliminate  $\omega_e(i)$  from Eq. (6.14) by putting  $J_{bs} = 0$  (equilibrium condition), and next using the linearized expansions of the functions  $N(i-1, t)$  and  $N^0(i-1)$  and the approximation  $l(i-1) \approx l(i)$ , as well as the derivative  $\partial N^0(i)/\partial i$  (from Eq. (6.8)), we are led to the flux equation in the form

$$(6.16) \quad J_{bs}(i, t) = -\omega_c l(i) \left[ \frac{N(i, t)}{kT} \frac{\partial \Delta F_{bs}(i)}{\partial i} + \frac{\partial N(i, t)}{\partial i} \right].$$

Substituting  $J_{bs}$  to the continuity equation and solving the resulting differential equation under the conditions  $\partial N(i, t)/\partial t = 0$  and  $N(\infty) = 0$ , we arrive at the non-equilibrium surface density of the clusters on the grain boundary

$$(6.17) \quad N(i) = N_0 S_{\text{het}} \exp \left[ -\frac{\Delta F_{bs}(i)}{kT} \right] \left\{ 1 - \frac{1}{2} (\alpha k T \Phi)^{-1/2} (2\Delta U + kT \ln H) \sin \theta \right. \\ \left. \times \exp \left( -\frac{\Delta F_{bs}^*}{kT} \right) \int_1^i \frac{1}{l(i)} \exp \left[ \frac{\Delta F_{bs}(i)}{kT} \right] di \right\}.$$

Insertion of Eq. (6.17) into Eq. (6.14) delivers finally the separated heterogeneous peripheral-growth-determined nucleation rate of microcracks in a steady state

$$(6.18) \quad J_{bs} = \frac{1}{2} N_0 S_{\text{het}} (2\Delta U + kT \ln H) \omega_c (\alpha k T \Phi)^{-1/2} \sin \theta \exp \left( -\frac{\Delta F_{bs}^*}{kT} \right).$$

These results (Eqs. (6.17) and (6.18)) are different from those obtained in ref. [11] since the release of the strain energy is now included in the total formation energy of a cluster  $\tilde{\Delta F}_{bs}(i)$ .

## 7. Coupling of the two mechanisms in the heterogeneous nucleation

We are now in a position to find the total coupled flux of heterogeneous clusters on the grain boundary. However, in the presence of both the surface and peripheral-growth mechanisms we do not know the coupled formation energy of clusters and can not postulate the equilibrium distribution function  $N^0(i)$ . Therefore, we start at once from the kinetics and the flux equation, basing our considerations on ref. [16].

Denoting the coupled heterogeneous nucleation rate on the grain boundary by  $J_{gs}(i, t)$  we can write the net flow of cap-shaped vacancy clusters in the form

$$(7.1) \quad J_{gs}(i, t) = J_{bg}(i, t) + J_{bs}(i, t) = N(i-1, t)P_c S(i-1) - N(i, t)P_e(i)S(i) \\ + N(i-1, t)\omega_c l(i-1) - N(i, t)\omega_e(i)l(i), \quad i \geq 2,$$

In both acting fluxes the growth mechanisms are entirely different. The flux  $J_{bg}$  is due to the surface addition of single elements from the vacancies dispersed inside the grain and, similarly as in the homogeneous process, is governed mainly by the supersaturation  $S_{ho}$  and by that part of the surface area of individual clusters  $S(i)$  which is in contact with the grain space. On the other hand, the flux  $J_{bs}$  being controlled by the peripheral growth through the surface transport of advacancies along the boundary depends chiefly on the corresponding surface supersaturation  $S_{het}$  and on the circumference of the base of an  $i$ -mer  $l(i)$ . These two different mechanisms, treated separately in Sects. 5 and 6, are now coupled under the classical assumption that the clusters increase or decrease only by capturing or losing one vacancy at a time independently of the mechanism by which it is accomplished. Simultaneous adding or losing two or more vacancies has a very small probability and is neglected.

Using the equilibrium conditions in which both the component fluxes  $J_{bg}$  and  $J_{bs}$  disappear, and putting in the first flux  $N(i, t) = N^0(i, \Delta F_{bg})$  and in the second one  $N(i, t) = N^0(i, \Delta F_{bs})$ , we are able to eliminate  $P_e(i)$  and  $\omega_e(i)$  from Eq. (7.1). Further treatment follows the same procedure as in the last two sections so that we can take advantage of Eqs. (5.19) and (6.16). Thus

$$(7.2) \quad J_{gs}(i, t) = - \left\{ [P_c S(i) + \omega_c l(i)] \frac{\partial N(i, t)}{\partial i} + \left[ \frac{P_c S(i)}{kT} \frac{\partial \Delta F_{bg}(i)}{\partial i} + \frac{\omega_c l(i)}{kT} \frac{\partial \Delta F_{bs}(i)}{\partial i} \right] N(i, t) \right\}.$$

Next, the equation of continuity which for the case considered is of the shape

$$(7.3) \quad \frac{\partial N(i, t)}{\partial t} + \frac{\partial}{\partial i} [J_{bg}(i, t) + J_{bs}(i, t)] = 0,$$

must be solved under the steady state condition  $\partial N(i, t)/\partial t = 0$ . This yields the differential equation for the stationary non-equilibrium distribution function  $N(i)$

$$(7.4) \quad J_{gs}(i, t) = (P_c S + \omega_c l) \frac{\partial N(i)}{\partial i} + \frac{1}{kT} \left( P_c S \frac{\partial \Delta F_{bg}}{\partial i} + \omega_c l \frac{\partial \Delta F_{bs}}{\partial i} \right) N(i) = C,$$

with a constant  $C$ .

The general solution of this nonhomogeneous equation has the form

$$(7.5) \quad N(i) = \exp\left(-\frac{1}{kT} \int_1^i \frac{P_c S \frac{\partial \Delta F_{bg}}{\partial i} + \omega_c l \frac{\partial \Delta F_{bs}}{\partial i}}{P_c S + \omega_c l} di\right) \\ \times \left[ N(1) + C \int_1^i \frac{1}{P_c S + \omega_c l} \exp\left(\frac{1}{kT} \int_1^i \frac{P_c S \frac{\partial \Delta F_{bg}}{\partial i} + \omega_c l \frac{\partial \Delta F_{bs}}{\partial i}}{P_c S + \omega_c l} di\right) \right],$$

where the integral in the exponent can be evaluated to give

$$(7.6) \quad \tilde{\Delta F}_{gs}(i) = \int_1^i \frac{P_c S \frac{\partial \Delta F_{bg}}{\partial i} + \omega_c l \frac{\partial \Delta F_{bs}}{\partial i}}{P_c S + \omega_c l} di \\ = \left\{ \Delta F_{bg}(i) - \frac{3kT \ln H}{D^3} \left[ \frac{D^2}{2} i^{2/3} - Di^{1/3} + \ln(Di^{1/3} + 1) \right] \right\} \\ - \left\{ \Delta F_{bg}(1) - \frac{3kT \ln H}{D^3} \left[ \frac{D^2}{2} - D + \ln(D+1) \right] \right\}.$$

Here,

$$(7.7) \quad D = \frac{P_c S(i)}{\omega_c l(i)} i^{-1/3} = \left(\frac{3}{4\pi}\right)^{1/3} \frac{P_c}{\omega_c} \left(\frac{V_v}{\Phi}\right)^{1/3} \frac{1 - \cos\theta}{\sin\theta},$$

and  $\Delta F_{bg}(i)$ ,  $\Delta F_{bg}(1)$ , and  $H(\varepsilon)$  are given by Eqs. (5.10)<sub>1,2</sub> and (6.6), respectively.

In equilibrium  $J_{gs}(i, t) = 0$ ,  $N(i) = N^0(i)$  and Eq. (7.4) becomes a homogeneous equation ( $C = 0$ ) solution of which yields the equilibrium distribution of clusters

$$(7.8) \quad N^0(i) = N^0(1) \exp\left[-\frac{\Delta F_{gs}(i)}{kT}\right],$$

where  $\tilde{\Delta F}_{gs}$ , given by Eq. (7.6), constitutes the total combined energy of formation of an  $i$ -mer in the coupled heterogeneous process involving both the surface and peripheral mechanisms of growth.  $\tilde{\Delta F}_{gs}$  is clearly a sum of two terms

$$(7.9) \quad \tilde{\Delta F}_{gs}(i) = \Delta F_{gs}(i) - \Delta F_{gs}(1),$$

where the first term is a size-dependent part of the formation energy

$$(7.10) \quad \Delta F_{gs}(i) = \Delta F_{bg}(i) - \frac{3kT \ln H}{D^3} \left[ \frac{D^2}{2} i^{2/3} - Di^{1/3} + \ln(Di^{1/3} + 1) \right],$$

and the second one

$$(7.11) \quad \Delta F_{gs}(1) = \Delta F_{bg}(1) - \frac{3kT \ln H}{D^3} \left[ \frac{D^2}{2} - D + \ln(D+1) \right],$$

is the mixing entropy contribution ( $-\Delta F_{bg}(1) = -kT \ln(N_0/N^0(1))$ ), and the effect of coupling. Similarly as in Sects. 4, 5 and 6, the total combined free energy of formation of the monomer itself is evidently zero,  $\tilde{\Delta F}_{gs}(1) = 0$ .

In view of Eqs. (7.8), (7.6) and (7.10) the equilibrium surface density of vacancy clusters finally reads

$$(7.12) \quad N^0(i) = N_0 \exp \left\{ -\frac{3 \ln H}{D^3} \left[ \frac{D^2}{2} - D + \ln(D+1) \right] \right\} \exp \left[ -\frac{\Delta F_{gs}(i)}{kT} \right].$$

Since

$$(7.13) \quad \left[ \frac{\partial \Delta F_{gs}(i)}{\partial i} \right]_{i=i_{gs}^*} = \left[ \frac{\partial \Delta F_{bg}(i)}{\partial i} \right]_{i=i_{gs}^*} - \frac{kT \ln H}{Di_{gs}^{*1/3} + 1} = 0,$$

and

$$(7.14) \quad \left[ \frac{\partial^2 \Delta F_{gs}(i)}{\partial i^2} \right]_{i=i_{gs}^*} = -\frac{2}{3} (36\pi)^{1/3} V_0^{2/3} \Phi^{1/3} \alpha i_{gs}^{*-4/3} + \frac{kTD \ln H i_{gs}^{*-2/3}}{3(Di_{gs}^{*1/3} + 1)^2} < 0,$$

the function  $\Delta F_{gs}(i)$  has a maximum

$$(7.15) \quad \Delta F_{gs}(i_{gs}^*) = \Delta F_{gs}^* = (36\pi)^{1/3} V_0^{2/3} \Phi^{1/3} \alpha i_{gs}^{*2/3} - 2\Delta U i_{gs}^* - \frac{3kT \ln H}{D^3} \left[ \frac{D^2}{2} i_{gs}^{*2/3} - Di_{gs}^{*1/3} + \ln(Di_{gs}^{*1/3} + 1) \right]$$

at the critical cluster composed of  $i_{gs}^*$  vacancies

$$(7.16) \quad i_{gs}^* = (8i_{bs}^*)^{-1} D^{-3} i_{bg}^* \{ i_{bs}^{*1/3} D - 1 + [(i_{bs}^{*1/3} D - 1)^2 + 4i_{bg}^{*-1/3} i_{bs}^{*2/3} D]^{1/2} \}^3.$$

It should be mentioned that, in general,  $D$  turns out to be a very small number, and since

$$(7.17) \quad \lim_{D \rightarrow 0} \frac{1}{D^3} \left[ \frac{D^2}{2} i^{2/3} - Di^{1/3} + \ln(Di^{1/3} + 1) \right] = \frac{i}{3},$$

$\Delta F_{gs}(i)$  and  $i_{gs}^*$  assume asymptotic values

$$(7.18) \quad \lim_{D \rightarrow 0} \Delta F_{gs}(i) = \Delta F_{bs}(i),$$

and

$$(7.19)^{(2)} \quad \lim_{D \rightarrow 0} i_{gs}^* = i_{bs}^*.$$

Coming back to the non-equilibrium distribution of clusters (Eq. (7.5)) we can write it now, in view of the integral (7.6) and Eq. (7.9), in the form

$$(7.20) \quad N(i) = \exp \left[ -\frac{\Delta F_{gs}(i) - \Delta F_{gs}(1)}{kT} \right] \left\{ N(1) + C \int_1^i \frac{1}{P_c S + \omega_c l} \times \exp \left[ \frac{\Delta F_{gs}(i) - \Delta F_{gs}(1)}{kT} \right] di \right\}.$$

Addition of the boundary condition  $N(\infty) = 0$  enables us to determine the constant  $C$  and gives the particular solution for the function  $N(i)$

$$(7.21) \quad N(i) = N_0 S_{\text{het}} \exp \left\{ -\frac{3 \ln H}{D^3} \left[ \frac{D^2}{2} - D + \ln(D+1) \right] - \frac{\Delta F_{gs}(i)}{kT} \right\} K(i),$$

(2) cf. Tables 2, 3 and 4 in Sect. 10.

where

$$(7.22) \quad K(i) = 1 - \frac{\int_1^i \frac{1}{P_c S + \omega_c l} \exp\left[\frac{\Delta F_{gs}(i)}{kT}\right] di}{\int_1^\infty \frac{1}{P_c S + \omega_c l} \exp\left[\frac{\Delta F_{gs}(i)}{kT}\right] di}$$

It is evident that  $0 \leq K(i) \leq 1$ .

Combination of Eq. (7.21) with Eq. (7.12) gives the relation between  $N(i)$  and  $N^0(i)$

$$(7.23) \quad N(i) = K(i) S_{het} N^0(i).$$

Eq. (7.21) is then substituted into Eq. (7.2), delivering the total steady state nucleation rate

$$(7.24) \quad J_{gs}(i, t) = J_{gs} = \frac{N_0 S_{het} \exp\left\{-\frac{3 \ln H}{D^3} \left[\frac{D^2}{2} - D + \ln(D+1)\right]\right\}}{\int_1^\infty \frac{1}{P_c S + \omega_c l} \exp\left[\frac{\Delta F_{gs}(i)}{kT}\right] di} = \text{const.}$$

Expanding  $\Delta F_{gs}(i)$  into Taylor series around  $i_{gs}^*$  and replacing  $S(i)$  and  $l(i)$  by  $S(i_{gs}^*)$  and  $l(i_{gs}^*)$ , the integral appearing in the denominator of Eqs. (7.22) and (7.24) can be approximated by the method shown in Sect. 4. This leads us to the final form of the coupled heterogeneous nucleation rate of microcracks on the grain boundaries

$$(7.25) \quad J_{gs} = \left(\frac{\pi}{6}\right)^{1/6} N_0 S_{het} \omega_c (kT)^{-1/2} \left(\frac{V_v}{\Phi}\right)^{1/3} \sin \theta \times [2i_{bg}^{*1/3} i_{gs}^{*-2/3} \Delta U (Di_{gs}^{*1/3} + 1)^2 - kTD \ln H]^{1/2} \times \exp\left\{-\frac{3 \ln H}{D^3} \left[\frac{D^2}{2} - D + \ln(D+1)\right] - \frac{\Delta F_{gs}^*}{kT}\right\}.$$

Similarly we can evaluate the coefficient  $K(i)$ , appearing in Eqs. (7.21) and (7.22), so that the final shape of the distribution function  $N(i)$  reads

$$(7.26) \quad N(i) = N_0 S_{het} \exp\left\{-\frac{3 \ln H}{D^3} \left[\frac{D^2}{2} - D + \ln(D+1)\right] - \frac{\Delta F_{gs}(i)}{kT}\right\} \times \left\{1 - \left(\frac{\pi}{6}\right)^{1/6} \omega_c (kT)^{-1/2} \left(\frac{V_v}{\Phi}\right)^{1/3} \sin \theta [2i_{bg}^{*1/3} i_{gs}^{*-2/3} \Delta U (Di_{gs}^{*1/3} + 1)^2 - kTD \ln H]^{1/2} \times \exp\left(-\frac{\Delta F_{gs}^*}{kT}\right) \int_1^i \frac{1}{P_c S + \omega_c l} \exp\left[\frac{\Delta F_{gs}(i)}{kT}\right] di\right\}.$$

If in Eq. (6.1) we put  $f_b \approx f_g \approx 0$  then  $S_{het} = S_{no}$  and  $H(\epsilon) = 1$ . In this case it is easy to see that  $\Delta F_{gs} = \Delta F_{bg} = \Delta F_{bs}$ ,  $i_{gs}^* = i_{tg}^* = i_{bs}^*$ , and the heterogeneous process is not coupled. Consequently, the flux  $J_{gs}$  presents the simple sum

$$(7.27) \quad J'_{gs} = J_{gs}(H = 1) = J_{bg}(H = 1) + J_{bs}(H = 1) = N_0 S_{no} (\alpha kT \Phi)^{-1/2} \times [P_c V_v (1 - \cos \theta) \alpha + \omega_c \Delta U \sin \theta] \exp\left(-\frac{\Delta F_{bg}^*}{kT}\right),$$

and the number of vacancies in the critical aggregate is

$$(7.28) \quad i_{gs}^{*'} = i_{gs}^*(H = 1).$$

## 8. Global steady state nucleation rate

Consider finally the entire grain of our observed internal region of the strained polycrystal. When all the fluxes are active in the formation of various classes of both homo and heterogeneous clusters we can write a balance equation for the steady state global nucleation rate  $J_0$

$$(8.1) \quad J_0 V_g = J_g V_g + J_{gs} S_g,$$

where  $V_g$  and  $S_g$  are volume and surface area of the grain, respectively, the homogeneous flux  $J_g$  is given by Eq. (4.29) and the coupled heterogeneous one  $J_{gs}$  by Eq. (7.25).

In Eq. (8.1) the product  $J_0 V_g$  means the sum of all the microcracks formed in the grain per unit time irrespectively of their shape or type. Consequently, it includes the homogeneous clusters generated within the grain space as well as the heterogeneous ones nucleated on the grain boundary.

From Eq. (8.1)  $J_0$  can be easily found

$$(8.2) \quad J_0 = J_g + J_{gs} \frac{S_g}{V_g}.$$

## 9. Conventional microfracture criterion

In the analysis of the course of fracture three main stages of the process can be distinguished. The first one is the microfracture stage in which stable microcracks of the size of atomic order are formed. In the second stage their further growth (or perhaps joining) to macroscopic dimensions of the order of a Griffith crack ( $\approx 1\mu$ ) takes place. Finally, the third one is the macrofracture stage in which the macrocracks (called simply cracks) propagate further leading immediately to the actual fracture. While for the first stage the present hypothesis can be applied, for the second one another theory should be introduced. The last cracking process (third stage) can follow the existing continuum hypotheses in which, however, the pre-existence of the crack is assumed a priori. One of such theories is the Griffith theory of brittle fracture in which the dependence of the potential energy of the sample with a crack on the initial length of the crack  $l$  is very similar to the relation between the energy of formation of a new phase  $i$ -mer in a supersaturated system and the size of the  $i$ -mer. Consequently, from the energy point of view there is a close analogy between the micro and macrofracture mechanisms. Moreover, in both cases there exists an instability of the equilibrium (thermodynamic or mechanical) since the corresponding energies instead of minimum values, as in the case of ordinary stable equilibrium, attain some maximum values.

From the above it follows that individual stages of the fracture process are separated by two energy thresholds, each corresponding to suitable fracture mechanism. They may



be called the microfracture and the macrofracture thresholds, respectively. The former is determined by the critical size  $i^*$  of a microcrack (or by the corresponding strain  $\varepsilon^*$ ), and the latter by the critical crack length  $l_{cr}$  (or by the corresponding critical strain  $\varepsilon_{cr}$ ).

Now, a formal convention concerning a critical value of the global nucleation rate,  $J_0^*$ , should be introduced to get a conceivably invariant measure of approaching the strain after which a crack of Griffith length can be originated. This means that the microfracture threshold is reached and the microfracture stage is terminated. At this strain stable microvoids, ready for further spontaneous growth, are generated. However, in most of the known phase transformation processes the period of time during which the actual number of the new phase nuclei is formed is short and difficult to determine precisely by either measurement or calculation [26]. Consequently, the nucleation frequency can be established only theoretically. Fortunately, the nucleation rate is so sensitive to the supersaturation that one may specify a critical supersaturation,  $S^*$ , below which nucleation rate is negligible ( $J \approx 0$ ) and above which it is very high ( $J \approx \infty$ ). For these reasons the critical supersaturation should correspond to the rate of nucleation having only some perceptible value, and it is generally agreed that meaningful data on homogeneous as well as heterogeneous nucleation in vapours and liquids are reported as supersaturations  $S^*$  corresponding to  $J \approx 1$  nucleus per sec and  $\text{cm}^3$  or  $\text{cm}^2$ . For metals such an agreement cannot be accepted. To establish a possibly invariant microfracture criterion for metals it seems that it should be connected with the dimensions of the grains. If we now assume that the supersaturation increases sufficiently slowly so that the induction period to establish a steady state of the system<sup>(3)</sup>  $\tau_1 \ll 1$  s [22, 26, 27], the following conventional microfracture criterion for uniaxially strained metals may be proposed: The global nucleation rate  $J_0^*$  yielding one arbitrary microcrack nucleus per second in the smallest grain is critical.

Thus, assuming the grain as a sphere with the diameter  $\delta_{\min}$  and volume  $V_{g\min}$ , we have

$$(9.1) \quad J_0^* = \frac{1}{V_{g\min}} = \frac{6}{\pi\delta_{\min}^3} \frac{\text{nuclei}}{\text{cm}^3\text{s}}$$

For this number of microcrack nuclei we should find a critical strain  $\varepsilon_0^*$ .

<sup>(3)</sup> Non-steady state nucleation theories consider the time period required to build up a steady state distribution of clusters immediately after a given supersaturation is imposed upon the system. During this induction time interval (called also time-lag, incubation time or delay time) the nucleation rate is time dependent, and no nucleation may take place before this period expires, whereas afterwards steady state is rapidly attained. In this way the induction time is separated from time to grow to observable size. The transient nucleation rate,  $J(t)$ , was approximately found in the form [30–32]

$$J(t) = J \exp\left(-\frac{\tau_1}{t}\right),$$

where  $J$  is the steady state nucleation rate,  $\tau_1$  is the induction time, and  $t$  is the observation time in a nucleation experiment.

For almost all cases of interest  $\tau_1$  is so small compared to the observation time  $t$  that  $J(t) \approx J$ . Moreover, it is reported in most papers that  $\tau_1 \ll 1$  s [22, 26, 27, 32]. It is worth noting, however, that because of comparatively slow rates of diffusion in condensed systems the induction period in solids may in some cases be considerably longer than in vapours and liquids [33], particularly when a system is suddenly made supersaturated.

Similar procedure can be formally applied also to isolated homogeneous and heterogeneous nucleations to find the corresponding critical strains  $\varepsilon_g^*$ ,  $\varepsilon_{bg}^*$ ,  $\varepsilon_{bs}^*$  and  $\varepsilon_{gs}^*$ . For each separated heterogeneous nucleation on the grain boundary we have to use  $1/S_{g\min}$  instead of  $1/V_{g\min}$  in Eq. (9.1).

## 10. Numerical estimates

In order to get an idea on quantitative results of the theory some numerical estimates for three metals: aluminium, copper, and  $\alpha$ -iron were computed. It should be stressed, however, that because of very sparse and uncertain data the calculations can only furnish very rough quantitative estimations.

Using the conventional criterion (9.1) with the grain diameter  $\delta_{\min} = 2.245 \times 10^{-3}$  cm (ASTM No 8), and corresponding nucleation rates, Eqs. (8.2), (4.29), (7.25), critical strains were found for several temperatures. To calculate the quantity  $\Delta U(\varepsilon)$  it was assumed in Eq. (3.1) that  $m = 1$ ,  $n = 10$ ,  $a \approx 8.5 \times 10^{-19}$  erg cm. The contact angle  $\theta$  was evaluated from the formula  $\cos\theta = E_a/[\alpha\pi(3V_v/4\pi)^{2/3}] - 1$  [34], and the probability factors

Table 1. Material constants used in the calculations

| Constant                         | Aluminium                | Copper                   | $\alpha$ -Iron           | Ref.                 |
|----------------------------------|--------------------------|--------------------------|--------------------------|----------------------|
| $R_0(\text{cm})$                 | $4.0496 \times 10^{-8}$  | $3.6149 \times 10^{-8}$  | $2.8665 \times 10^{-8}$  | [35]                 |
| $\alpha(\text{erg}/\text{cm}^2)$ | 900                      | 1200                     | 1400                     | estimated from [36]  |
| $U_f(\text{erg})$                | $1.0400 \times 10^{-12}$ | $1.4400 \times 10^{-12}$ | $1.4400 \times 10^{-12}$ | [37]<br>[38]<br>[39] |
| $U_m(\text{erg})$                | $9.9200 \times 10^{-13}$ | $1.6640 \times 10^{-12}$ | $1.0560 \times 10^{-12}$ | [37]<br>[40]         |
| $U_{sd}(\text{erg})$             | $5.7600 \times 10^{-13}$ | $8.3200 \times 10^{-13}$ | $6.8800 \times 10^{-13}$ | estimated            |
| $E_a(\text{erg})$                | $6.0000 \times 10^{-13}$ | $6.0000 \times 10^{-13}$ | $7.6000 \times 10^{-13}$ | estimated            |

Table 2. Values of  $\varepsilon_g^*$ ,  $i_g^*$ ,  $\varepsilon_0^* \approx \varepsilon_{gs}^*$ ,  $i_{bg}^*$ ,  $i_{gs}^* \approx i_{bs}^*$  for aluminium ( $J_g^* = J_0^* = 1.688 \times 10^8$  nuclei/cm<sup>3</sup> s).

| Al                | Minimal grain, $\delta_{\min} = 2.245 \times 10^{-3}$ cm |         |   |            |                             |
|-------------------|--|---------|---|------------|-----------------------------|
|                   | Homogeneous nucleation                                   |         | Global nucleation $\approx$<br>Heterogeneous nucleation |            |                             |
|                   | $\varepsilon_g^*$  | $i_g^*$ | $\varepsilon_0^* \approx \varepsilon_{gs}^*$            | $i_{bg}^*$ | $i_{gs}^* \approx i_{bs}^*$ |
| $T^\circ\text{K}$ |  |         |   |            |                             |
| 300               | 0.0972   | 4.08    | 0.0914  | 3.38       | 4.31                        |
| 400               | 0.0901   | 5.92    | 0.0827  | 5.56       | 6.23                        |
| 500               | 0.0846   | 8.12    | 0.0774  | 7.75       | 8.46                        |
| 600               | 0.0801   | 10.65   | 0.0735  | 10.08      | 10.98                       |
| 800               | 0.0734   | 16.63   | 0.0679  | 15.15      | 16.77                       |
| 900               | 0.0708   | 20.02   | 0.0658  | 17.86      | 20.01                       |

Table 3. Values of  $\varepsilon_g^*$ ,  $i_g^*$ ,  $\varepsilon_0^* \approx \varepsilon_{gs}^*$ ,  $i_{bg}^*$ ,  $i_{gs}^* \approx i_{bs}^*$  for copper.

( $J_g^* = J_0^* = 1.688 \times 10^8$  nuclei/cm<sup>3</sup> s for  $\delta_{\min} = 2.245 \times 10^{-3}$  cm, and  
 $J_0^* = 1.910 \times 10^3$  nuclei/cm<sup>3</sup> s for  $\delta_{\text{av}} = 0.1$  cm).

| Cu                | Minimal grain, $\delta_{\min} = 2.245 \times 10^{-3}$ cm |         |   |            |                             | Average grain, $\delta_{\text{av}} = 0.1$ cm            |            |                             |
|-------------------|--|---------|---|------------|-----------------------------|---|------------|-----------------------------|
|                   | Homogeneous nucleation                                   |         | Global nucleation $\approx$<br>Heterogeneous nucleation |            |                             | Global nucleation $\approx$<br>Heterogeneous nucleation |            |                             |
| $T^\circ\text{K}$ | $\varepsilon_g^*$  | $i_g^*$ | $\varepsilon_0^* \approx \varepsilon_{gs}^*$            | $i_{bg}^*$ | $i_{gs}^* \approx i_{bs}^*$ | $\varepsilon_0^* \approx \varepsilon_{gs}^*$            | $i_{bg}^*$ | $i_{gs}^* \approx i_{bs}^*$ |
| 300               | 0.1045   | 2.44    | 0.0929  | 2.81       | 2.81                        | 0.0893  | 3.41       | 3.41                        |
| 400               | 0.0958   | 3.73    | 0.0854  | 4.26       | 4.26                        | 0.0819  | 5.25       | 5.25                        |
| 500               | 0.0889   | 5.37    | 0.0798  | 6.01       | 6.01                        | 0.0764  | 7.48       | 7.48                        |
| 600               | 0.0835   | 7.35    | 0.0753  | 8.02       | 8.03                        | 0.0721  | 10.04      | 10.05                       |
| 800               | 0.0755   | 12.22   | 0.0688  | 12.77      | 12.82                       | 0.0656  | 16.03      | 16.08                       |
| 900               | 0.0725   | 15.06   | 0.0663  | 15.42      | 15.53                       | 0.0635  | 19.39      | 19.49                       |
| 1000              | 0.0699   | 18.14   | 0.0642  | 18.28      | 18.44                       | 0.0615  | 22.95      | 23.14                       |
| 1300              | 0.0640   | 28.71   | 0.0593  | 27.64      | 28.23                       | 0.0568  | 34.69      | 35.33                       |

in Eqs (3.9), (6.7) were set to be  $p_g = 1/6$  and  $p_b = 1/4$ . Further, we put  $N_0 \approx 1/d^2 \text{ cm}^{-2}$ ,  $d = R_0 \text{ cm}$ , and  $\nu = 10^{13} \text{ s}^{-1}$ . The remaining material constants are listed in Table 1. They are taken from references, shown in Table 1, or assumed, recognising that this is only a rough approximation. Critical strains and numbers of vacancies in critical aggregates for different nucleation processes and various temperatures are shown in Tables 2, 3, and 4.

It is to be noted that the resulting  $\varepsilon^*$  and  $i^*$  depend on the grain size. The conventional criterion (9.1) gives the highest critical strains  $\varepsilon^*$  and the smallest critical sizes  $i^*$  of a microcrack. To estimate the effect of the grain size on these two important quantities the calculations were additionally carried out for copper with the average grain of the diameter  $\delta_{av} = 0.1 \text{ cm}$  [41]. The results for both grains are given in Table 3.

**Table 4.** Values of  $\varepsilon_g^*$ ,  $i_g^*$ ,  $\varepsilon_0^* \approx \varepsilon_{gs}^*$ ,  $i_{bg}^*$ ,  $i_{gs}^* \approx i_{bs}^*$  for  $\alpha$ -iron ( $J_g^* = J_0^* = 1.688 \times 10^8 \text{ nuclei/cm}^3 \text{ s}$ ).

| Fe- $\alpha$      | Minimal grain, $\delta_{\min} = 2.245 \times 10^{-3} \text{ cm}$ |         |   |            |                             |
|-------------------|--|---------|---|------------|-----------------------------|
|                   | Homogeneous nucleation   |         | Global nucleation $\approx$<br>Heterogeneous nucleation |            |                             |
| $T^\circ\text{K}$ | $\varepsilon_g^*$  | $i_g^*$ | $\varepsilon_0^* \approx \varepsilon_{gs}^*$            | $i_{bg}^*$ | $i_{gs}^* \approx i_{bs}^*$ |
| 300               | 0.0940   | 3.23    | 0.0853  | 3.13       | 3.20                        |
| 400               | 0.0879   | 4.51    | 0.0794  | 4.50       | 4.55                        |
| 500               | 0.0829   | 6.05    | 0.0748  | 6.07       | 6.12                        |
| 600               | 0.0787   | 7.82    | 0.0712  | 7.85       | 7.92                        |
| 800               | 0.0724   | 12.01   | 0.0656  | 11.92      | 12.07                       |
| 900               | 0.0699   | 14.40   | 0.0635  | 14.19      | 14.41                       |
| 1000              | 0.0677   | 16.98   | 0.0616  | 16.58      | 16.90                       |
| 1700              | 0.0576   | 39.35   | 0.0530  | 36.68      | 38.37                       |

For comparison the computations were also repeated for the global nucleation rate  $J_0^* = 1/V_g = 1 \text{ nucleus/cm}^3 \text{ s}$ .  $V_g = \Sigma V_{g\min} = 1 \text{ cm}^3$  denotes the total volume of all the grains contained within  $1 \text{ cm}^3$ , under the assumption that all of them are minimal grains ( $\delta_{\min} = 2.245 \times 10^{-3} \text{ cm}$ ) so that  $S_g/V_g = \Sigma S_{g\min}/\Sigma V_{g\min} = 2672.6 \text{ cm}^{-1}$ . The corresponding strains are presented below in Table 5.

**Table 5.** Values of  $\varepsilon_0^* \approx \varepsilon_{gs}^*$  for  $J_0^* = 1 \text{ nucleus/cm}^3 \text{ s}$ .

| $T^\circ\text{K}$ | Al   | Cu   | Fe- $\alpha$                                 |
|-------------------|--|--|--|
|                   | $\varepsilon_0^* \approx \varepsilon_{gs}^*$ | $\varepsilon_0^* \approx \varepsilon_{gs}^*$ | $\varepsilon_0^* \approx \varepsilon_{gs}^*$ |
| 300               | 0.0815                                       | 0.0848                                       | 0.0788                                       |
| 400               | 0.0749                                       | 0.0775                                       | 0.0729                                       |
| 500               | 0.0702                                       | 0.0722                                       | 0.0685                                       |
| 600               | 0.0667                                       | 0.0681                                       | 0.0650                                       |
| 800               | 0.0617                                       | 0.0623                                       | 0.0598                                       |
| 900               | 0.0597                                       | 0.0600                                       | 0.0579                                       |
| 1000              |  | 0.0581                                       | 0.0561                                       |
| 1300              |  | 0.0538                                       |  |
| 1700              |  |  | 0.0484                                       |

To estimate the effect of coupling in the heterogeneous nucleation the simple sum  $J'_{gs} = J_{bg} + J_{bs}$  (Eq. 7.27) was also used to calculate the corresponding critical strains  $\varepsilon_{gs}^{*}$  and numbers of vacancies in critical clusters  $i_{gs}^{*}$  for all three metals and the minimal grain (Table 6). The distributions of separate fluxes  $J_{bg}$  and  $J_{bs}$  are also given in Table 6.

Table 6. Values of  $\varepsilon_{gs}^{*}$ ,  $i_{gs}^{*}$ ,  $J_{bg}$ ,  $J_{bs}$  for aluminium, copper, and  $\alpha$ -iron.

$$(J_{gs}^{*} = 1/S_{g \min} = 6.315 \times 10^4 \text{ nuclei/cm}^2 \text{ s for } \delta_{\min} = 2.245 \times 10^{-3} \text{ cm}).$$

| Metal          | $T^\circ\text{K}$ | $\varepsilon_{gs}^{*}$ | $i_{gs}^{*}$ | $J_{bg}$<br>nuclei/cm <sup>2</sup> s | $J_{bs}$<br>nuclei/cm <sup>2</sup> s |
|----------------|-------------------|------------------------|--------------|--------------------------------------|--------------------------------------|
| Aluminium      | 300               | 0.0876                 | 4.18         | 4.4                                  | 63152.8                              |
|                | 400               | 0.0811                 | 6.15         | 17.2                                 | 63130.1                              |
|                | 500               | 0.0762                 | 8.39         | 68.1                                 | 63091.5                              |
|                | 600               | 0.0724                 | 10.91        | 208.8                                | 62948.3                              |
|                | 800               | 0.0667                 | 16.68        | 1069.0                               | 62080.3                              |
|                | 900               | 0.0645                 | 19.91        | 1953.3                               | 61202.8                              |
| Copper         | 300               | 0.0929                 | 2.81         | $7.8 \times 10^{-4}$                 | 63147.6                              |
|                | 400               | 0.0854                 | 4.26         | 0.03                                 | 63150.7                              |
|                | 500               | 0.0797                 | 6.01         | 0.4                                  | 63150.9                              |
|                | 600               | 0.0753                 | 8.03         | 2.4                                  | 63147.6                              |
|                | 800               | 0.0687                 | 12.81        | 33.0                                 | 63118.1                              |
|                | 900               | 0.0662                 | 15.52        | 85.3                                 | 63067.1                              |
|                | 1000              | 0.0641                 | 18.43        | 188.4                                | 62963.6                              |
|                | 1300              | 0.0591                 | 28.21        | 1077.5                               | 62069.8                              |
| $\alpha$ -Iron | 300               | 0.0850                 | 3.19         | 7.3                                  | 63142.4                              |
|                | 400               | 0.0792                 | 4.54         | 28.9                                 | 63131.5                              |
|                | 500               | 0.0747                 | 6.12         | 94.4                                 | 63052.4                              |
|                | 600               | 0.0711                 | 7.91         | 247.9                                | 62905.9                              |
|                | 800               | 0.0655                 | 12.06        | 1057.9                               | 62102.9                              |
|                | 900               | 0.0633                 | 14.39        | 1837.9                               | 61308.4                              |
|                | 1000              | 0.0614                 | 16.89        | 2932.8                               | 60218.0                              |
|                | 1700              | 0.0526                 | 38.32        | 18204.8                              | 44945.7                              |

Although the numerical results of the theory are very approximate ones, some essential quantitative conclusions can be derived. In the first place it turns out that the effect of the homogeneous flux  $J_g$  on the global nucleation rate  $J_0$  is negligibly small and can be disregarded. Consequently, the global nucleation rate depends almost exclusively on the coupled heterogeneous mechanism and  $\varepsilon_0^* \approx \varepsilon_{gs}^*$ , which is shown in the above tables. This result supports earlier statements that the vacancy clusters observed are nucleated heterogeneously [4, 5, 27]. In the second place it comes out that the simple sum  $J'_{gs} = J_{bg} + J_{bs}$  can be a good approximation for the coupled heterogeneous nucleation rate  $J_{gs}$ . The approximation is better for copper and  $\alpha$ -iron than for aluminium (cf. Tables 2, 3, 4 and 6). Moreover, in the sum  $J'_{gs}$ , the calculations show the predominant effect of  $J_{bs}$  for lower temperatures and rising influence of  $J_{bg}$  for higher temperatures, which for  $\alpha$ -iron at  $T = 1700^\circ\text{K}$  reaches 29% (Table 6). This indicates that the distribution of

both fluxes  $J_{bg}$  and  $J_{bs}$  is not that simple as was stated in ref. [12]. In coupled heterogeneous nucleation the contribution of the surface-controlled mechanism ( $J_{bg}$ ) is even greater.

## 11. Conclusions and final remarks

The vacancy hypothesis of microfracture of strained metals has been further extended by taking into account the strain energy as part of the free energy of formation of vacancy clusters. Moreover, quantitative estimates provide an idea of the numerical values resulting from the theory and deliver important inferences.

In view of the idealized model of the metal, disregarding the effect of other kinds of defects, some formally introduced physical quantities, and many unknown or uncertain data, the vacancy mechanism of microfracture of strained metals has mainly theoretical character. Moreover, it is not quite clear whether the actual supersaturations caused by the strain in real metals are not too low to nucleate a vacancy-microcrack. In the present theory the critical global nucleation rate requires supersaturations ranging from a rather impossibly high value of  $10^8$  to around 3.5. These are dropping very rapidly with rising temperature so that beginning from  $800^\circ\text{K}$  they do not exceed 50. On the other hand, it was reported [4, 5, 42, 43] that the highest supersaturation at which voids are produced amounts to merely 1.01. Such a low supersaturation was estimated from diffusion experiments without any external tension applied. It is of interest to note here that in the paper [44] a critical vacancy supersaturation for pore formation during the interdiffusion of copper and zinc was found to be about 1.5, which is contrary to the above statements. Much higher supersaturations at which voids are generated appear also in irradiated metals [2, 3] where, however, the presence of interstitials cannot be neglected because of the competing effects of interstitials and vacancies on the void formation. It should be added that high-energy radiation frequently induces high supersaturations not only of vacancies and interstitials but also of dissolved inert gas atoms which may co-precipitate into voids. The internal gas pressure in the gas-containing void embryos lowers the formation energy of the embryos, decreasing thereby the supersaturation needed to nucleate a critical void. Under such circumstances internal pressure, aided by the strain due to tension, facilitates the origination of microvoids and should be incorporated in the free energy of void formation [23].

In spite of the doubts about the sufficiency of vacancy supersaturation, a number of papers [1, 5, 45] is in agreement with the suggestion that stable void nuclei are induced by the tensile stress. Moreover, the vacancy hypothesis gives a theoretical explanation of the beginning of the microfracture process and the nature of origination of submicroscopic cracks which can initiate the formation of a Griffith crack. It should be stressed here that the strain  $\varepsilon$ , which appears in the equations of the theory, denotes not the average linear strain of the crystal but rather the highly increased local strain occurring at the boundaries of each vacancy cluster. This increased strain reduces the activation energy of vacancy motion and accelerates the nucleation process. Thus, despite the small value of the mean strain, large local strains appearing inside the crystal favour the growth of a microcrack

nucleus and vacancy collections which are still unstable. Unfortunately, the strain concentration coefficients are not sufficiently known, and the value of the average strain of the crystal corresponding to the critical strain  $\varepsilon^*$  can be either determined by an experiment or estimated only approximately.

The formation of a microcrack nucleus results here from the application of an elastic strain to the metal and in the first microscopic stage is a reversible process. On unloading the vacancy supersaturation decreases, the nuclei cease to be stable and disintegrate, and the metal returns to the original state. When the unloading process is very rapid the healing of microcracks may proceed slower than their growth. On the other hand, once the growing nucleus has reached a macroscopic size, its further growth is irreversible; otherwise, no crack could exist in free of loaded bodies.

### Acknowledgements

The author expresses his thanks to Professor A. ZIABICKI for valuable discussions and to Dr. M. KOŚC for performing the numerical computations.

### References

1. J. N. GREENWOOD, D. R. MILLER, J. W. SUITER, *Acta Met.*, **2**, 250, 1954.
2. K. C. RUSSELL, *Acta Met.*, **19**, 753, 1971.
3. J. L. KATZ, H. WIEDERSICH, *J. Chem. Phys.*, **55**, 1414, 1971.
4. R. W. BALLUFFI, *Acta Met.*, **2**, 194, 1954.
5. R. W. BALLUFFI, L. L. SEIGLE, *Acta Met.*, **3**, 170, 1955.
6. J. KRZEMIŃSKI, *Arch. Mech. Stos.*, **21**, 3, 215, 1969.
7. J. KRZEMIŃSKI, *Arch. Mech. Stos.*, **21**, 4, 429, 1969.
8. J. KRZEMIŃSKI, *IFTR Reports* [in Polish], 44, 1974.
9. J. KRZEMIŃSKI, *Arch. Mech.*, **25**, 6, 903, 1973.
10. J. KRZEMIŃSKI, *ZAMM*, **56**, T 122, 1976.
11. J. KRZEMIŃSKI, *Proc. of Second Int. Symp. on Defects, Fracture and Fatigue*, Mont Gabriel, Quebec, Canada, June 1982. Ed. by Martinus Nijhoff Publishers, The Hague 1983.
12. G. M. POUND, M. T. SIMNAD, L. YANG, *J. Chem. Phys.*, **22**, 1215, 1954.
13. B. K. CHAKRAVERTY, *J. Phys. Chem. Solids.*, **28**, 2413, 1967.
14. R. D. GRETZ, *Surface Sci.*, **6**, 468, 1967.
15. R. A. SIGSBEE, *J. Crystal Growth*, 13/14, 135, 1972.
16. A. ZIABICKI, *IFTR Reports*, 4, 1977.
17. В. Я. ПИНЕС, *Журнал Технической Физики*, **25**, 8, 1399, 1955.
18. R. BECKER, W. DÖRING, *Annalen der Physik*, **24**, 5, 719, 1935.
19. W. DÖRING, *Z. Physik. Chem. (B)*, **36**, 371, 1937.
20. M. VOLMER, *Kinetik der Phasenbildung*, Steinkopff, Dresden und Leipzig 1939.
21. J. FRENKEL, *Kinetic theory of liquids*, Dover Publications, Inc., New York 1955.
22. J. H. HOLLIMON, D. TURNBULL, *Progress in metal physics*, Vol. 4, p. 333. Ed. by B. Chalmers and R. King, Pergamon Press, London 1953.
23. K. C. RUSSELL, *Acta Met.*, **20**, 899, 1972.
24. J. WEERTMAN, J. R. WEERTMAN, *Elementary dislocation theory*, Macmillan, London 1967.
25. V. HALPERN, *Brit. J. Appl. Phys.*, **18**, 163, 1967.
26. J. P. HIRTH, G. M. POUND, *Condensation and evaporation*, Pergamon Press, Oxford 1963.

27. T. L. DAVIS, J. P. HIRTH, *J. Appl. Phys.*, **37**, 2112, 1966.
28. A. ZIABICKI, *J. Chem. Phys.*, **48**, 4368, 1968.
29. J. LOTHE, G. M. POUND, *J. Chem. Phys.*, **36**, 2080, 1962.
30. J. B. ZELDOVICH, *Acta Physicochimica, USSR*, **18**, 1, 1, 1943.
31. K. C. RUSSELL, *Acta Met.*, **17**, 1123, 1969.
32. J. FEDER, K. C. RUSSELL, J. LOTHE, G. M. POUND, *Advan. Phys. (Phil. Mag. Suppl.)*, **15**, 57, 111, 1966.
33. D. TURNBULL, *Trans. AIME*, **175**, 774, 1948.
34. B. LEWIS, *Thin Solid Films*, **1**, 85, 1967.
35. R. W. G. WYCKOFF, *Crystal structure*, Vol. 1, Second Ed., John Wiley, New York 1963.
36. A. KOCHENDÖRFER, *Arch. für das Eisenhüttenwesen*, **25**, 351, 1954.
37. A. SEEGER, H. MEHRER, *Vacancies and interstitials in metals*, Proc. Int. Conf., Jülich, Germany, 1968. Ed. by A. Seeger, D. Schumacher, W. Schiling, J. Diehl, North-Holland, Amsterdam 1970.
38. F. G. FUMI, *Phil. Mag.*, **46**, 1007, 1955.
39. Б. С. БОКШТЕЙН, С. З. БОКШТЕЙН, А. А. ЖУХОВИЦКИЙ, *Термодинамика и кинетика диффузий в твердых телах*, Металлургия, Москва, 1974.
40. R. A. JOHNSON, *Phys. Rev.*, **134**, A 1329, 1964.
41. L. H. VAN VLACK, *Elements of materials science*, Addison-Wesley, Massachusetts, London 1959.
42. J. A. BRINKMAN, *Acta Met.*, **3**, 140, 1955.
43. E. S. MACHLIN, *Trans. AIME, J. of Met.*, **206**, 106, 1956.
44. R. RESNICK, L. SEIGLE, *Trans. AIME*, **209**, 87, 1957.
45. D. HULL, D. E. RIMMER, *Phil. Mag.*, **4**, 673, 1959.

POLISH ACADEMY OF SCIENCES  
INSTITUTE OF FUNDAMENTAL TECHNOLOGICAL RESEARCH.

Received January 26, 1983.